CORPORACIÓN MEXICANA DE INVESTIGACIÓN EN MATERIALES

POSTGRADUATE STUDIES DIVISION

COMIMSA

POSGRADO INTERINSTITUCIONAL
CIENCIA Y TECNOLOGIA

FAULT PREDICTION AND DIAGNOSIS IN SQUIRREL CAGE INDUCTION MOTORS WITH INTELLIGENT CONTROL SYSTEMS

THESIS

PRESENTS

DAVID ALEJANDRO FERNÁNDEZ TAVITAS

MASTER IN SCIENCE AND TECHNOLOGY
IN ADVANCED MANUFACTURING SYSTEMS

SALTILLO, COAHUILA. DECEMBER 2015

FAULT PREDICTION AND DIAGNOSIS IN SQUIRREL CAGE INDUCTION MOTORS WITH INTELLIGENT CONTROL SYSTEMS

By

David Alejandro Fernández Tavitas

Thesis

Presented to the Interinstitutional Postgraduate in Science and Technology

Location

Corporación Mexicana de Investigación en Materiales S. A. de C.V

As a partial requirement to obtain the Academic Degree

Master in Science and Technology in Advanced Manufacturing Systems

Interinstitutional Postgraduate in Science and Technology COMIMSA CONACYT

Saltillo, Coahuila. December 2015

Corporación Mexicana de Investigación en Materiales

Human Development Management

Postgraduate Studies Division

The undersigned members of the Tutorial Committee recommend that the thesis **"FAULT PREDICTION AND DIAGNOSIS IN SQUIRREL CAGE INDUCTION MOTORS WITH INTELLIGENT CONTROL SYSTEMS "**, realized by the student **DAVID ALEJANDRO FERNÁNDEZ TAVITAS** register number **1306MA3102** to be accepted for the defense as Master in Science and Technology in Advanced Manufacturing Systems.

Tutorial Committee

Dr. Melvyn Álvarez Vera
Thesis Director

Dr. Pedro Pérez Villanueva
Company tutor

Dr. Felipe Arturo Reyes Valdés
General Coordinator of Postgraduate Studies
COMIMSA

Corporación Mexicana de Investigación en Materiales

Human Development Management

Postgraduate Studies Division

The undersigned members of the Jury of the grade exam of the student **DAVID ALEJANDRO FERNÁNDEZ TAVITAS**, once read and reviewed the thesis titled **"FAULT PREDICTION AND DIAGNOSIS IN SQUIRREL CAGE INDUCTION MOTORS WITH INTELLIGENT CONTROL SYSTEMS "**, accept that that reviewed and corrected thesis is submitted by the student to aspire to the degree of Master of Science and Technology in **Advanced Manufacturing Systems** during the exam of the corresponding Grade.

and for the record we sign this on the 10th day of December 2015.

Dr. Juan Pablo Nieto González
President

Dr. Felipe Hernández Rodríguez
Secretary

Dr. Melvyn Álvarez Vera
Vocal

Dedicated

To God
To my parents:
María del Carmen and Raúl Juan

To my Brother:
Raúl

To Gissel

To my friends

Acknowledgements

Thanks to God for giving me life and health to achieve this goal.

Thanks to my two examples of life, my parents, who provided me the tools needed to succeed, for showing me that family is the most important thing in life and for showing me that there is nothing in life that cannot be achieved with effort.

To my brother, in whom I always find support, in whom I always find a friend.

To Gissel, for motivating me every day to be a better person.

To my friends, for making this project a great life experience.

Special appreciation to the support received during my master to two important institutions of science and technology in this country; COMIMSA (Corporación Mexicana de Investigación en Materiales) and CONACyT (Consejo Nacional en Ciencia y Tecnología) because without them, my progress and academic development would not have been possible.

Autobiographical summary

David Alejandro Fernández Tavitas was born in Saltillo Coahuila on July 9, 1991. He graduated as a Mechatronic engineer of Instituto tecnológico de Saltillo in February 2013 and made its industrial stay as an intern in the company COMIMSA (Corporación Mexicana de de Investigación en Materiales SA de CV). He was developed as a student in the Master of Advanced Manufacturing Systems in Corporación Mexicana de Investigación en Materiales S.A. de C.V. for 2 years between the period September 2013 - December 2015, under the project: Fault Prediction and Diagnosis in squirrel cage induction motors with Intelligent Control Systems to earn the degree of Master in Science. David dominates different languages such as Spanish and English.

Synthesis

Nowadays, one of the main objectives of the companies is based in the generation of monitoring and control systems which ensure the proper function of the processes, resulting in the reduction of costs occasioned by faults on the devices. In order to provide the companies the tools to achieve these objectives, the following work presents a methodology for fault detection and diagnosis in squirrel cage induction motors, with the use of the techniques Motor Square Current Signature Analysis (MSCSA) and fuzzy logic systems. The project covers the following topics: Development of the work bench for fault simulation and load system. Development of the interface for analysis and data processing. Development of the system for fault detection and diagnosis. The system was developed for the detection of 3 faults; Mechanical faults generated by eccentricities (static and dynamic) and electrical faults generated by broken bars in the rotor and / or voltage unbalance. Finally, in order to show the efficiency of the proposed methodology, the project was tested and validated on 2 squirrel cage induction motors of 1 and 3 hp, respectively.

Contents

List of Tables

List of Figures

Chapter 1

Introduction

In order to complete the objectives of developing and transferring technology, the project should cover the next topics: knowledge of soft computing techniques like: fuzzy logic in order to develop a system of control and fault diagnosis. But also, techniques for signal analysis (like Fourier transform and Fast Fourier Transform) will be needed too. In this research the techniques of Artificial Intelligence and Classical Control techniques for modelling, identification, monitoring, and fault diagnosis of complex systems are analyzed [1]. The development of a system able to work with the presence of noise and fault tolerant control are proposed, like in manufacturing systems or electrical systems to name a few. The presence of combinations and correlations between similar analogue or digital variables. presence of noise. linear or non-linear characteristics are commonly present which represent a challenge in order to make a diagnosis or control. It is remarked the use of artificial intelligence techniques in order to perform intelligent control and monitoring systems. This is because the design of the machines that make the systems that currently exist are trying to emulate the behavior of human systems and / or animals. so that in order to control and diagnostics of these systems using only traditional control methods is impossible to achieve given the large amount of information handled. the large number of correlated variables and the presence of uncertainty [2]. Given this. is proposed the research based in the handle of historical data of the process combined with soft computing and statistical techniques. to develop an intelligent control and monitoring system based on the historical data of the process.

Chapter 2

Research Problem

In recent times, in the industries is more often to see automatized processes with a big machinery variety like robots, working center, transportation etc. All of these basing their function on induction motors for their reliability and simplicity of their construction. In the actuality induction motors are the most used electrical machine in the industry for the simplicity in their installation and maintenance. The constant use of these motors make them so susceptible to fail. In this regard, it is necessary to check them within a certain period of time. The problem is that some techniques need to stop the motor to evaluate their condition, triggering high costs during the stop in the production line. That is why it is wanted to implement a continuous diagnostic system that can give information about the conditions of the motor, and that could be used to predict a fault in the main components (broken rotor bar and eccentricities), allowing to correct the failure before the motor stops working. All this without the need to stop the motor and in consequence the production line.

2.1 Research questions

1. Which are the mechanical and electrical faults more frequently presented on electrical induction motors and which are the possible solutions in order to correct them?

2. Is it possible the creation of constant monitoring system to detect faults on induction motors able to work on line without the need to stop the motor to make a proper diagnosis?

3. Is it possible the development of a methodology, based on Motor Square Current

Signature Analysis (MSCSA) and Soft Computing techniques, able to detect patterns that represent the existence of electrical and mechanical faults on electrical induction motors?

4. Is it possible the creation of an interface to detect faults on induction motors able to work in presence of noise?

2.2 Hypothesis

With the use of MSCSA and soft computing techniques, it is possible the creation of a continuous monitoring and control system to analyze the signals online, that reveal the behavior of the motor in full operation, able to work with the presence of noise, with the purpose of predict electrical(broken rotor bars) and mechanical(eccentricities) faults before they occur.

2.3 Main objective

To develop a methodology for fault prediction in electrical induction motors applying MSCSA and soft computing techniques based on the treatment of historical data of the process.

2.3.1 Specific objectives

- To develop a sturdy monitoring and control system able to work in presence of noise.

- To perform a constant monitoring system and control in order to avoid the stop of the motor.

2.3.2 Delimitations

1. The program is delimited to the detection and diagnosis of faults specifically broken rotor bars and eccentricities, without reaching on the automation and the correction of these.

2. The methodology will be developed just for squirrel cage induction motors.

2.4 Justification

In many industrial processes control function is performed by an operator (human). This is who decides when and how to manipulate variables in order to get a continuous and efficient production line. Productive efficiency involves the constant increase in production levels of installed equipment, improving product quality, lower production costs and safety for workers and equipment. To achieve this goals, it is necessary that the production processes are performed at the highest possible speed and the control variables are at the lowest value allowed. Because of these requirements the industry has required the use of new and more complex processes that often cannot be control by an operator. That is why intelligent control and monitoring systems arise as an answer to the industrial needs, in order to get production standards at the highest level of quality, and the lowest maintenance costs [3].

Chapter 3

State of the art

Nowadays companies have searched for ways to invest their business in improvements for their industrial processes. One of the topics that has taken more importance is the prevention of faults in the machinery of the system in order to extend the life of the mechanisms and thereby to generate a higher rate of production reducing time for repair and / or maintenance. Based on this, the detection and diagnosis of faults has grown significantly aiming to have systems and processes in control impacting directly on the economy of the company.

One of the devices presented in that processes is the induction motor by its versatility and easy installation, for that reason several techniques has emerged in order to address this problem. There are a lot of problems that a motor can presents, like faults on the stator windings, voltage unbalances, bearing problems, eccentricity faults, broken rotor bars and others. However, two of the most usually presented problems on the motors are eccentricity faults (static, dynamic or mixed) and broken rotor bars. One of the first to confront this topic was Acosta [1]. He present a review of some techniques to fault detection like Park Vector, Negative sequence and Stator current analysis to detect variations or patterns that indicate the presence of a fault. After the experimentation he presents thatthe technique used would depend directly to the system that is going to be analyzed, giving a little advantage to the analysis of the stator current.

Subsequently, Mehrjou [4] realized a complete review of the existing techniques for the fault detection and diagnosis, presenting the advantages and disadvantages of some different techniques. He presents analysis by vibrations, thermal analysis and analysis to the stator current. Every technique presented its advantage in the analysis of some specific parts of the motor, for example vibration analysis presents better results identifying eccentricities that the others, the problem is that vibrations do not detect electrical faults [5]. Then thermal analysis presented an advantage to vibrations for its multiple fault detection, bearings, eccentricities, shortcircuits and others, the problem of thermal analysis is that instrumentation has an elevated cost besides it presented problems to diagnose under multiple fault present. The last technique presented was the analysis to the stator current. This technique presents good results to detect eccentricities, broken rotor bars, stator and bearing faults, the instrumentation required for the analysis has an affordable price and the simplicity of the technique made the stator current analysis one of the most used techniques for induction motor fault detection. The analysis of the stator current is named Motor Current Signature Analysis (MCSA) and consists basically in 3 steps:

- First step consists on the acquisition of the current from one of the motor phases, which represents the behavior of the magnetic fields of the motor.

- Second step consists on the transformation of the current from time domain to the frequency domain based on Fourier transform. The goal of this transformation is to detect patterns that in time domain is not possible to detect.

- Third step consists on the analysis of those patterns to diagnose the type of the fault. The patterns used for the analysis are the presence of harmonics located at certain frequency. Depending on the frequency of the harmonic, it is possible to determine the type of the fault [6]. One prove of the efficiency of MCSA technique was developed by Neti [7], who analyze a motor under accelerated life test. The motor was installed to be in extreme conditions of ventilation and it was turned on and off constantly by 8 days. The results were collected every day to detect the state of the motor and based in the data collected, the systems preview that motor was going to fail in the 8th day as happened.

MCSA technique enables the system to detect different types of faults like eccentricities and broken rotor bars. To detect these faults, it is necessary to determine the frequency location of the harmonics and the amplitude of them. Rico [8] presents the frequency location of the harmonics depending on the type of the fault. For example, to determine the presence of an eccentricity fault in the frequency analysis, the harmonics should be presented at frequencies

$$f_{ecc} = f_s(1 \pm k(\frac{1-s}{p})) \tag{3.1}$$

Where:

f_{ecc} is the frequency of the fault
f_s is the supply frequency
s is the slip (difference between the mechanical speed and electrical speed)
p is the number of poles
k is an integer

Moreover, other authors reports that Eccentricity fault presents harmonics at frequencies $f_{ecc} = f_r \pm f_s$. This information was tested and validated by Rajalakshmi [9] with a model based in multiple coupled circuit approach and 2D Modified Winding Function Theory. On the other hand, for the analysis of broken rotor bars, the frequency harmonics are located to the sidebands of the supply frequency located at:

$$f_{brb} = (1 \pm ks)f_s \tag{3.2}$$

f_{brb} is the frequency of the fault
f_s is the supply frequency
s is the slip
k is an integer.

These harmonics provide the necessary information to detect broken rotor bars when the motor is working at full load [10], [11]. However, Bruzesse [12] reports one point to take in count when analyzing broken rotor bars. MCSA presents good results to detect a low number of broken rotor bars, nevertheless, when is analyzed a high number of broken bars, the technique presents an efficiency lost. For that reason Bruzesse presents that the maximum amplitude value of the harmonics gets when the consecutive number of broken rotor bars reach next relation $N_{brb} = \frac{N_{bars}}{N_{poles}}$. Subsequently, in order to solve that problem, Kumar [13] proposed an extra pattern for the classification. He showed that in addition to the presence of the harmonics present on the sides of the main frequency, the amplitude of the supply frequency is affected by the state of the rotor. As higher is the defect of the rotor, lower is the amplitude of the supply frequency harmonic.

Once solved the problem of the number of broken bars, only an issue misses to correct. The technique MCSA presents good results for the detection of faults at full or half load conditions, however when working under conditions of low load or no load, the effectiveness of the technique is greatly reduced [14]. For that reason, the next goal was to improve the resolution of the frequency spectrum. One of the techniques proposed was developed by Benbouzid [15]. It was proposed to obtain the motor current and then to resample it with the use of eigenvalues and eigenvectors to nullify the presence of noise in the frequency spectrum, the results obtained showed good results to improve the resolution of voltage unbalance patterns, nevertheless the technique was not proved for different types of fault patterns. Another technique proposed to improve the resolution of the current was the use of the Hilbert Transform. The technique is used to emphasize the local properties of the signal obtained. It consists in to reduce the negative frequency harmonics to zero and doubling the amplitude of the positive harmonics with respect of the original signal spectrum component. Even though the system presented improve on the resolution of the frequency spectrum, the technique continued presenting problems to detect faults under low load conditions [16] [17].

Jung [18] observed that the correct way to analyze the current system was not based in the improve the quality of frequency spectrum, the correct way to do it was with a correct sample selection for each type of fault. Subsequently Sahraoui [19] presented an algorithm called Relative Harmonic Indexes (RHI) It consisted in an auto searching system to detect harmonics on the frequency spectrum, and with them generate patterns for further analysis.

One point to be remarked is that Motor Current Signature Analysis is not an autonomous technique for fault detection and diagnosis, MCSA is dedicated to reveal frequency patterns for the fault detection, however, the presence of an operator is necessary to make a correct diagnosis. For that reason, several techniques of pattern classifications have emerged in order to generate a complete system of fault detection and diagnosis. The first methodology proposed was made it by Chaudhury [20]. It was proposed to combine MCSA with the statistical technique K-means. The methodology consisted in three steps: a) Data collection for normal operation for a certain period of time b) Generation of the cluster for normal operation c) Compare the data to detect abnormal harmonics. If the system identify harmonics out of the clusters, it sends an alert that the fault is present. The methodology presents good results for single faults. However the complex of the process, statistical techniques presents problems to identify multiple faults present.

Subsequently, in order to confront the complexity of the process, intelligent control systems emerged as a possible answer. Two different techniques were used in combination with MCSA to develop a precise fault detection and diagnosis system. The first of them was presented by Guedidi [21] who developed a methodology which combines MCSA and an Artificial Neural Network (ANN) to classify broken rotor bars in the induction motors. Results obtained showed the efficiency of the technique to detect single faults, but tests for multiple faults was not been developed. Consecutively, Nordin [22] presents an ANN-MCSA methodology for multiple types of faults. The patterns selected for the system were the frequency and amplitude of the odd harmonics from 1st to the 19th and the ANN was a Multi-Layer Perceptron. The results obtained shown the ability of the technique to identify single and multiple faults with a high percentage of precision. Nevertheless, the methodology carried the problems of the technique MCSA to identify faults under low load conditions.

The second intelligent technique proposed was Fuzzy systems. Pereira [23] presented a methodology for shortcircuits on the windings and Zouzou [24] for broken rotor bars. They estipulate 2 input variables for the detection: the position and the amplitude of the selected harmonics and one single output: the state of the motor. Based on the results obtained, it is possible to determine the efficiency of the technique taking in count two points. a) the system can handle the uncertainty related with the motor conditions, and b) the system can consider the experience of the operator to determine the amplitude of the harmonics.

However, one last point should be highlighted, the impact of the quality of the current in the analysis. Samaga [25] reports the influence of the voltage unbalance to the eccentricity detection. The problems in the quality of the current provoke that eccentricity harmonics increase, generating false alarms. For that reason a new pattern to recognize voltage unbalance was required. One alternative is presented by Shady [26]. It proposed a MCSA-ANN system to detect the presence of voltage unbalance on the system based on the information provided by the third subsequent harmonic. On the other hand, Fonseca [27] proposed the analysis of the Total Harmonic Distortion (THD) to detect bad quality in the supply current. The technique quantify the amplitude of the multiples harmonics and identify the distortion of the supply current. This technique presents precise information about the quality of the current, making the THD a powerful tool to detect voltage unbalances.

Finally, after the review of the literature there are propose some improvements to the project that will be developed. In the existent methodologies, the techniques were developed with the objective to predict one type of fault, either mechanical faults (eccentricities) or electrical faults (broken rotor bars), but not both on the same process, and if they are able to detect them, they present problems when it is needed to work under low load conditions. That is why it is wanted to implement a technique able to detect not just electric faults but also mechanical faults in the same analysis. To accomplish that goal the methodology is going to use the Technique Motor Square Current Signature Analysis (MSCSA). The technique was proposed by Pires [28] to identify broken rotor bars an eccentricity faults and bases its function in the same principle of MCSA, the difference of MSCSA is that the obtained current gets a pre-process to square it. The aim of this process is to duplicate the amplitude of the harmonics reducing the problems of MCSA to work under low load conditions. For the pattern classification, Fuzzy logic presented some specific characteristics like uncertainty handle and the ability to work with variables based on human experience, making the Fuzzy logic the suitable technique for the project.

Chapter 4

Theoretical Framework

4.1 Electric Motors

An electrical machine is a device that converts electrical energy into mechanical energy or mechanical energy into electrical energy. When this device is used to convert mechanical into electrical energy is named generator. When the device is used to convert electrical energy into mechanical is named motor. In the industry as in common life is easy to find these types of electrical machines like in fridges, fans, vacuums, blenders, air conditioning and others. All these has a simple answer, because electrical energy is an efficient source of energy, easy to manipulate and transmit long distances [29].

4.1.1 Clasification

Electric motors can be classified according to the current used in: Direct Current motors (DC), Alternate Current motors (AC) and universal motors (used for both types current).

- **Direct Current Motors**
  DC motor are used when the application where they are going to be used is important to control the speed and the rotation direction. These motors are mostly found in devices that works with batteries. In these motors is necessary to have the same number of poles in the stator and in the

rotor to work. They can be classified according to the type of excitation in: independent, serial, derivation, composed and permanent magnet (the magnetic field is produced by magnets instead of electromagnets.

– **Alternate Current Motors**

These motors are the most used on the industry, for the simplicity in their installation and maintenance, in the actuality these motor is the most used motor because they have good responding and they are able to work under unusual conditions. AC motors are classified in two more types, synchronous and asynchronous motors. In turn, AC motors are classified depending on the rotation speed, the rotor type and phase quantity [30].

* synchronous
* asynchronous
  - single-phase
  - auxiliary winding
  - short-circuited winding
  - universal
  - three-phase
  - winding rotor
  - short-circuited rotor

4.1.2 Three-Phase AC motors

Motor construction

The basic construction of an electric motor is mainly conformed by two parts, a fixed part called stator and a moving part called rotor.

Stator

Is the base operating element, allows the motor to have a star point where rotation can be started.There are two stator types:

* salient pole stator
* grooving stator

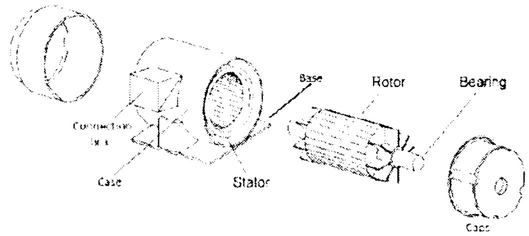

Figure 4.1: Motor parts
Adapted from [31]

Figure 4.2: Stator types
Adapted from [31]

Stator are mainly constructed by a set of steel sheets (called package), that have the ability to allow the pass of magnetic flux through them easily, creating the magnetic fields by stator and its windings.

- **Rotor**

  Is the mechanical transfer element, this part depends on the electrical to mechanical energy conversion. Rotors are a group of steel sheets to form a package, and can be essentially on three types depending on their application:

  * slotting rotor
  * salient pole rotor
  * squirrel cage rotor

Fundamentals of operation

Electrical motors base their function in the use of electrical fields, there are 3 basic principles that describe their operation:

An electric charge is induced trough a conductor generating a magnetic field around it.

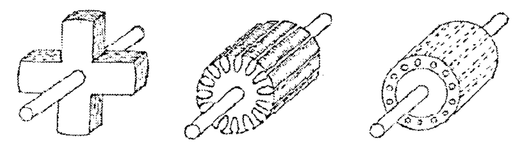

Figure 4.3: Rotor types
Adapted from [31]

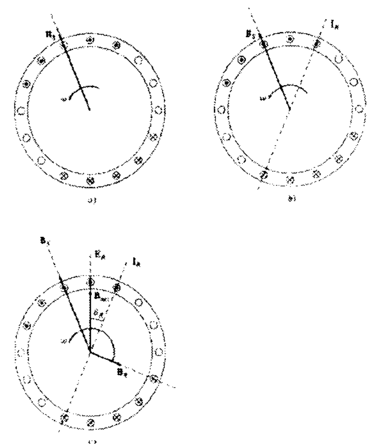

Figure 4.4: Fundamentals of induction motor operation
Adapted from [29]

Another conductor which is electrical inducted too, generates and opposite magnetic field to the first one.

- The repulsion force between both magnetic fields develop rotation movement which is then used for mechanical applications.

The operation principle is based on the rotating magnetic field that creates a three-phase alternating current. The motor is conformed by a pair of poles per phase with their corresponding windings, whose ends are joined in a common point. A three-phase balanced voltage system is applied at the start point of the windings, the currents flowing each time represents different positions.

For example, in Figure 4.4 is shown how the rotating field of the stator B_S induces voltage in the rotor bars, then the rotor voltage produces a current flow in the rotor that retard the voltage due to the inductance generated by itself, finally the rotor current produces a magnetic field in the rotor B_R at 90° behind her and

B_R interacts with B_{net} to produce a par in the opposite clockwise direction.

The resulting magnetic field rotates at a frequency of f revolutions per second. If the machine has p pairs of poles, the speed, in revolutions per minute, would be [29]

$$n_1 = \frac{120 \cdot f_1}{p} \tag{4.1}$$

4.1.3 Induction Motors

Once, having defined the basics of operation of an electric motor, it continues with the definition of the induction motor, which bases its operation on the same principle of rotation generated by magnetic fields, however, the induction motor does not require an external excitation applied to the rotor, it works directly with the flux generated by the stator.
The operation of the induction motor is based on the action of the rotating flow generated in the stator circuit flow induced on the rotor circuit currents. The rotating flux created by stator winding, short-circuit the rotor conductors, so that induced electromotive forces are generated. Assuming that rotor winding is closed, it is to understand that rotor is induced by electric currents. The mutual action of the rotating flow and the existing currents in the rotor conductors, causes electrodynamic forces on the conductors, generating the rotation on the rotor.

The voltage induced in a rotor bar of an induction motor depends on the speed the rotor with respect to the magnetic fields. To generate an electromotive force between the rotor bars, there must be a speed difference between the rotor speed and magnetic fields. This difference is called slip, and is defined as the difference between the synchronous speed and the rotor speed, also known as relative speed.

$$s = \frac{\omega_{sinc} - \omega_m}{\omega_{sinc}}(X100\%) \tag{4.2}$$

Equation 4.2 represents the calculation of the slip in percentage and is defined by the next values: s is the slip, ω_{sinc} is the speed of the magnetic fields and ω_m is the rotor mechanical speed in terms of angular speed ω (radians per second) [31].

4.2 Control

A control system is defined as a set of components that can regulate their own behavior or the behavior of another system in order to achieve a predetermined operation, with propose of reduce faults probabilities and obtain expected results. There are two types of control, open loop and closed loop control.

Open loop control system: are those where the control inputs are chosen without regard to the actual system outputs. The performance of such systems can only be guaranteed if the task remains the same for all time and can be duplicated repeatedly by a specific set of inputs.

Closed loop control system: are systems where the behavior of the system is observed by some sensory device, and the observations are feedback so that a comparison can be made about how well the system is behaving in relation to some desired performance [2].

4.2.1 Intelligent Control

Intelligent control systems are described as the development of control techniques and methodologies, with the objective to emulate important characteristics of the human intelligence:

- adaptation
- learning
- big data quantity manipulation

Intelligent control base its function in a number of techniques in order to solve problems that cannot be solved with classical control techniques. Among these problems are those where it is necessary to work with large amounts of data, as well as handling of uncertainty. It is important to remark that intelligent control systems efficiency depends greatly in the quantity and quality data of the process.

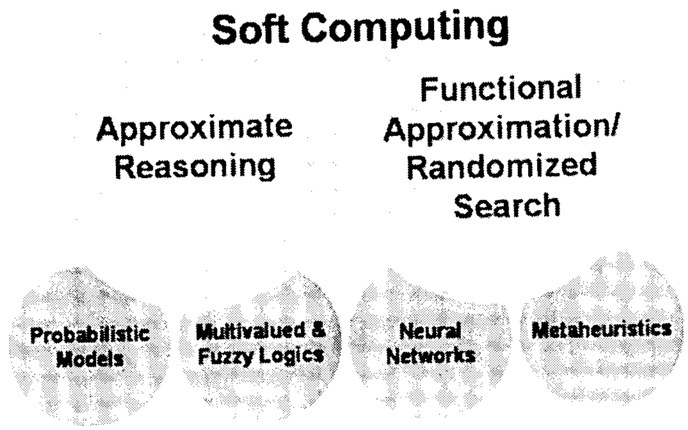

Figure 4.5: Soft computing Techniques

Soft computing techniques are divided in two main areas. Approximate reasoning and Functional approximation or Randomize search as it is shown on figure 4.5. This classification has in turn 4 subsections, who are the principal techniques of soft computing:

- Fuzzy Logic
- Probabilistic models
- Neural Networks
- Genetic algorithms

4.3 Fuzzy Logic

Fuzzy systems are knowledge-based or rule-based systems. The principle of a fuzzy system consists on the construction of series of IF-THEN rules or also called Fuzzy rules, where based on the experience or knowledge of the system, it is possible to establish a relation of the inputs in order to obtain a desired output An IF-THEN rule, consists in a series of steps in which is establish the result or response, depending on the action(s) that have occurred. For example:

"IF the speed of the car is high, THEN apply less force on the accelerator".

Where the words"high" and "less", are concepts that in first instance does not represent a nominal value, but in a Fuzzy system represents a value parameter, which is next explained.

As mentioned before, the rules of a fuzzy system, are not defined with the use of nominal values, but these values are related in order to generate an input parameter which is called "membership function".

4.3.1 Membership Function

A membership function is a universe of values which belong to a defined set. Consider X as a collection of values denoted by x, then a fuzzy set A in x is defined as a set of ordered pairs given by:

$$A = \{x, \mu_A(X)|x \in X\} \tag{4.3}$$

Where $\mu_A(x)$ is called the membership function MF for the fuzzy set A. The MF maps each element of x to a membership value between 0 and 1. It is obvious that if the value of the membership function $\mu_A(x)$ is restricted to either 0 or 1, then A is reduced to a classical set, and $\mu_A(x)$ is the characteristic function of A. Usually X is referred to as the universe of discourse, or simply the universe, and it may consist of discrete (ordered or unordered) objects or continuous space.

The construction of a fuzzy set depends on two things: the identification of a suitable universe of discourse and the specification of an appropriate membership function.

For example, in the case of the car, the values of "high" and "less" are next described:

Figure 1.6: MF for High

Figure 1.7: MF for Less

On the figure 1.6 can be observed that when the speed of the car is lower or equal to 40 mph, the membership grade is zero, when the speed of the car passes the value of 40mph, the degree of membership begins growing until reach 60mph, where the degree of membership reaches the value of 1. This represents that for this function, lower or equal velocities to 40mph has no high speed characteristics, values from 60mph and higher, are considered totally high speed, and the values between 40-60mph have certain percentage of high speed.

Figure 1.7 shows that the value"less" starts in zero, pass through 1 but ends in zero again, which can be interpreted that this function has just one area which represents the value"less", and the rest of the values higher can be defined as too much force.

As in the examples shown, the membership function of every value should not to have the same class, there are different classes of MF's depending on the complexity required. Next, a few classes of parametrized MF's are described:

Singleton Membership Function

The singleton MF maps a real valued point $x \in U$ into a fuzzy singleton A' in U, which has membership value 1 at a and 0 at all other points in U, that is:

$$\mu_{A'(x)} = \begin{cases} 1 & if \quad x = a \\ 0 & otherwise \end{cases} \tag{4.4}$$

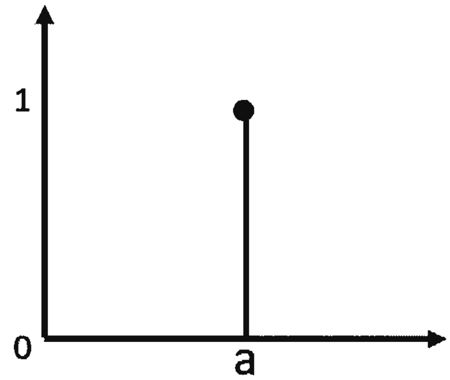

Figure 4.8: Singleton Membership Function

Triangular Membership function

The triangular MF maps $x \in U$ into a fuzzy set A' if the membership function has the following form:

$$\mu_{A'(x)} = \begin{cases} \frac{x-\alpha}{a-\alpha} & if \quad \alpha \leq x < a \\ \frac{\beta-x}{\beta-a} & if \quad a \leq x \leq \beta \\ 0 & otherwise \end{cases} \tag{4.5}$$

Where a is the center (peak), $\alpha > 0$ the left width and $\beta > 0$ the right width, this means, support is $(a - \alpha, a + \beta)$.

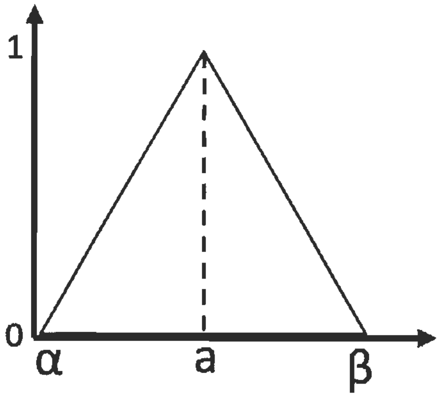

Figure 4.9: Triangular Membership Function

Trapezoidal Membership Function

The triangular MF maps $x \in U$ into a fuzzy set A' if the membership function has the following form:

$$\mu_{A'(x)} = \begin{cases} \frac{x-\alpha}{a-\alpha} & if \quad \alpha \leq x < a \\ 1 & if \quad a \leq x \leq b \\ \frac{\beta-x}{\beta-b} & if \quad b \leq x \leq \beta \\ 0 & otherwise \end{cases} \tag{4.6}$$

Where $[a, b]$ is the tolerance interval, $\alpha > 0$ the left width and $\beta > 0$ the right width, this means, support is $(a - \alpha, b + \beta)$.

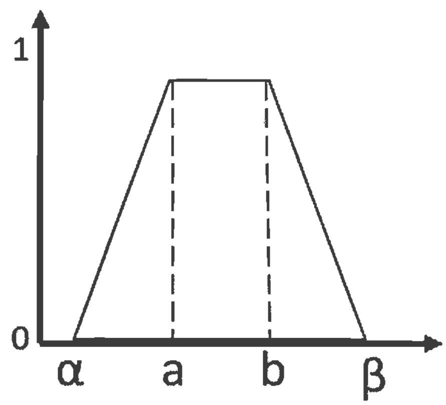

Figure 4.10: Trapezoidal Membership Function

4.3.2 Fuzzy Rule Base

Structure

A fuzzy rule base consists of a set of fuzzy IF-THEN rules. It is the heart of the fuzzy system in the sense that all other components are used to implement these rules in a reasonable and efficient manner. Specifically, the fuzzy rule base comprises the following fuzzy IF-THEN rules:

$$Ru^{(l)} : IF\ x_1\ is\ A_1^l\ and\ ...\ and\ x_n\ is\ A_1^n\ THEN\ y\ is\ B^l \tag{4.7}$$

Where A_i^l are fuzzy sets in $U_i \subset R$ and $V \subset R$ respectively, and $x = (x_1, x_2, ..., x_n)^T \in U$ and $y \in V$ are the input and output (linguistic) variables of the fuzzy system, respectively. Where M is the number of the rules in the fuzzy rule base; that is $l = 1, 2, ..., M$ in 4.7.

In fuzzy systems, human knowledge is represented in a fuzzy IF-THEN form, this means

Properties

A set of fuzzy IF-THEN rules is complete if for any $x \in U$, there exists at least one rule in the fuzzy rule base, say rule $Ru^{(1)}$ (in the form of (4.7)), such that:

$$\mu_{A_i^l}(x_i) \neq 0 \tag{4.8}$$

Intuitively, the completeness of a set of rules means that at any point in the input space there is at least one rule that "fires"; that is, the membership value of the IF part of the rule at this point is non-zero.
A set of fuzzy IF-THEN rules is consistent if there are no rules with the same IF parts but different THEN parts.
A set of fuzzy IF-THEN rules is continuous if there do not exist such neighbouring rules whose THEN part fuzzy sets have empty intersection. Intuitively, continuity means that the input-output behavior of the fuzzy system should be smooth.

There are a great gamma about fuzzy rules depending on the interpretation an the use of the operators (t-norms, s-norms and complements), however, one of the most used is the Mamdani implication, so next will be described:

Mamdani implication, uses the min or algebraic product in $p \rightarrow q = p \wedge q$.
This means, IF-THEN rule is interpreted as a fuzzy relation QM with the MF's

$$\mu_{Q_{MM}}(x, y) = min\left(\mu_{FP_1}(x), \mu_{FP_2}(y)\right) \tag{4.9}$$

or

$$\mu_{Q_{MP}}(x, y) = \mu_{FP_1}(x)\mu_{FP_2}(y) \tag{4.10}$$

4.3.3 Fuzzy Inference Engine

Although fuzzy rules represent the knowledge and control strategy of the system, when a specific input value is established, it is necessary to use a tool in order to calculate the result of the output variables. For this action it is necessary to use an inference machine, which is the responsible of generating a single set based on the stipulated rules, which have an individual output variable, aiming to obtain a joint response as the system output.

There are several inference engines, based on the needs of the system, however, two of the most used inference engines are next described: Mamdani(max-min) and Takagi Sugeno.

Mamdani Inference Engine

The fuzzy implication is modellde by Mamdani minimum operator and the sentence connective also is interpreted as origin the prepositions and defined by max operator.
The firing levels of the rules, denoted by α_i, $i = 1, 2$ are computed by

$$\alpha_1 = A_1(x_0) \wedge B_1(y_0), \alpha_1 = A_1(x_0) \wedge B_2(y_0) \tag{4.11}$$

The individual rule outputs are obtained by

$$C_1'(w) = (\alpha_1 \wedge C_1(w)), C_2'(w) = (\alpha_2 \wedge C_2(w)) \tag{4.12}$$

Then, the overall system output is computed by joining the individual rule outputs

$$C(w) = C_1'(w) \vee C_2'(w) = (\alpha_1 \wedge C_1(w)) \vee (\alpha_2 \wedge C_2(w)) \tag{4.13}$$

Finally, to obtain a deterministic control action, it is employed any defuzzification strategy.

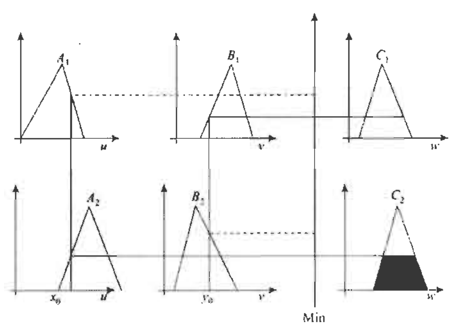

Figure 4.11: Inference with Mandani's Implication operator
(adapted from [2])

Takagi Sugeno Inference Engine

Sugeno and Takagi use the following architecture

R_1: if x is A_1 and y is B_1 then $z_1 = a_1x + b_1y$
also

R_2:	if x is A_2 and y is B_2 then $z_2 = a_2x + b_2y$
fact :	x is $\bar{x}_0$ and y is $\bar{y}_0$
Consequence:	z_0

The firing levels of the rules are computed by

$$\alpha_1 = A_1(x_0) \wedge B_1(y_0), \alpha_1 = A_1(x_0) \wedge B_2(y_0) \tag{4.14}$$

The individual rule output are derived from the relationship

$$z*_1 = a_1x_0 + b_1y_0, z*_2 = a_2x_0 + b_2y_0 \tag{4.15}$$

and the crisp control action is expressed as

$$z_0 = \frac{\alpha_1 z *_1 + \alpha_2 z*_2}{\alpha_1 + \alpha_2} \tag{4.16}$$

If we have n rules in the rule-base then the crisp control action is computed as

$$z_0 = \frac{\sigma_{i=1}^{n} \alpha_1 z*_1}{\sigma_{i=1}^{n} \alpha_i} \tag{4.17}$$

Where α_i denotes the firing level of the $i - th$ rule, $i = 1, ..., n$.

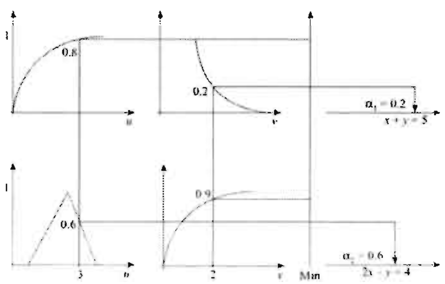

Figure 4.12: Inference with Takagi Sugeno Implication operator
(adapted from [2])

4.3.4 Defuzzification

Once, having obtained the output of the system, the response obtained is given into a fuzzy set, but in most of the control processes, the output desired should be given in to a nonfuzzy number, also called crisp. Consequently, one must defuzzify the output inferred from the fuzzy control algorithm, namely:

$$z_(0) = defuzzifier(C) \tag{4.18}$$

Where z_0 is the nonfuzzy control output and $defuzzifier$ is the defuzzification operator.

Defuzzification is a process to select a representative element form the fuzzy output C inferred from the fuzzy control algorithm.

The most often used defuzzification operators are:

Center of Area / Gravity

The defuzzifier value of a fuzzy set C is defined as its fuzzy centroid:

$$z_0 = \frac{\int zC(z)dz}{\int c(z)dz} \tag{4.19}$$

The calculation of the Center of Area defuzzified values is simplified if we consider finite universe of discourse W and thus discrete membership function $C(w)$, [32][2].

$$z_0 = \frac{\sigma x_j C(z_j dz)}{\sigma c(z_j)} \tag{4.20}$$

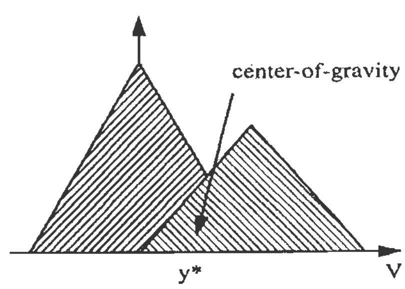

Figure 4.13: Center of Area defuzzification method
(adapted from [32])

First of Maxima

The defuzzified value of a fuzzy set C is its smallest maximizing element.

$$z_0 = min\{z|C(z) = maxC(w)\} \tag{4.21}$$

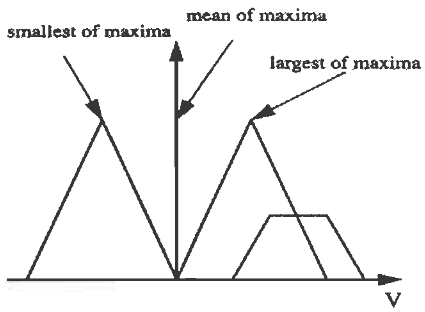

Figure 4.14: First of Maxima defuzification method (adapted from [32])

4.4 Motor Current Signature Analysis

Motor Current Signature Analysis (MCSA) is a technique which base its function on the monitoring of the stator current to detect sidebands around the supply frequency, identifying the type of the fault depending on the sidebands magnitude and location, for example eccentricity or broken rotor bars.

4.4.1 Fault Detection by MCSA

In order to detect faults with the use of Motor Current Signature Analysis it is necessary to obtain a frequency spectum which has important information about the behavior of the motor. In the spectral are showed important paterns like the supply frequency and sidebands which represents the type and the magnitude of the fault depending on the location and the amplitude of the harmonic [4].

4.4.2 Healthy State

If it is considered an ideal motor in power and voltage conditions it is possible to observe an amplitude increase on the supply frequency trough the next formula 4.22.

$$i_a(t) = I_{max}cos(wt) \tag{4.22}$$

Where I_{max} is the maximum value of the fundamental supply phase current.

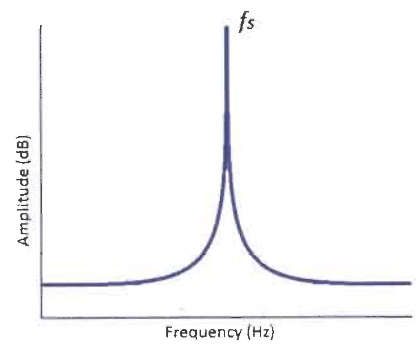

Figure 4.15: Stator Current Spectrum in Healthy State

4.4.3 Broken Rotor Bar

If an induction motor with broken rotor bars is considered, it is possible to detect patterns on the frequency spectral. In first instance, broken rotor bars produce variations in the magnetic field of the motor, which results in the appearance of harmonics of rotating field, which induces magneto-motive forces which eventually lead to the appearance of harmonics in the supply current to the motor. Consequences of these are mechanical vibration and loss of torque or driving torque [18]. It is possible to observe a peak on the supply frequency and two sidebands around it. To obtain this spectral it is necessary to process the phase current with the next equation.

$$i_a(t) = I_{max}cos(wt) + I_{lsb}cos[(1 - 2s)wt] + I_{usb}cos[(1 + 2s)wt] \tag{4.23}$$

Where:
I_{max} is the maximum value of the fundamental supply phase current.
I_{lsb} is the maximum value of the current lower sideband component.
I_{usb} is the maximum value of the current upper sideband component.

In the figure 4.16 is possible to observe an example of the frequency spectrum which highlight a peak on the supply frequency and sidebands at the frequencies $(1-2s)f_s$ and $(1+2s)f_s$ respectively.

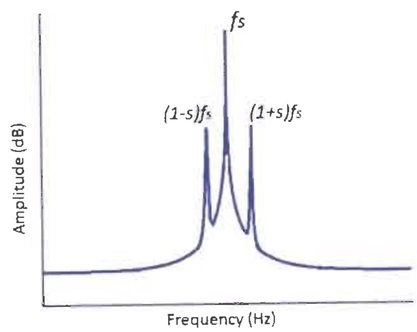

Figure 4.16: Stator Current Spectrum with broken rotor bar

4.4.4 Eccentricity

There is a gap between the rotor and the stator of the motor called "Air Gap". If the Air-Gap is not well distributed in the 360°, a fault known as eccentricity could be produced. There are basically two types, static in which the rotor is eccentric but fixed in a place; and dynamic eccentricity, in which the shaft has an unbalance and the rotor is rotating around the air gap. These faults cause unequal magnetic fields on the motor, that ultimately result in insulation faults and bearings faults [14]. In order to obtain this spectral, it is necessary to process the phase current with the next equation.

$$i_a(t) = I_{max}cos(\omega t) + I_{lsb}cos[(\omega - \omega_r)t] + I_{usb}[(\omega - \omega_r)t] \tag{4.24}$$

In the figure 4.17 is possible to observe an example of the frequency spectrum which highlight a peak on the supply frequency and sidebands at the frequencies $(f_s - f_r)$ and $(f_s + f_r)$ respectively.

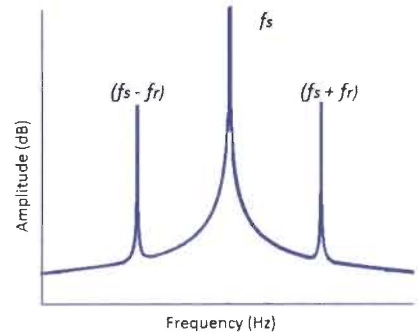

Figure 4.17: Stator Current Spectrum with Eccentricity

4.5 Motor Square Current Signature Analysis

Such as in MCSA, in this technique (MSCSA) a frequency analysis is performed on the stator current, however the technique presented uses the square of the current, which facilitates the detection of patterns indicating the existence of faults. The technique bases its methodology in 3 main steps. 1) Acquisition of the stator phase current in operation 2) processing the square of the current obtained by formula (4.25) ; and 3) Analysis of the square of the current through the frequency spectrum with the use of Fourier transform [28].

4.5.1 Normal Operation

The frequency spectrum for a healthy motor can be obtained by the processing of the stator current with the use of the next formula 4.25

$$i_a^2(t) = \frac{I_{max}^2}{2} + \frac{I_{max}^2 cos(\omega t)}{2} \tag{4.25}$$

Where:
I_{max} is the maximum value of the fundamental current.
ω is the angular frequency $\omega = 2\pi f_s$

In the obtained frequency spectrum it is possible to detect the fundamental frequency on $2f_s$ and a DC component as is showed on the next figure

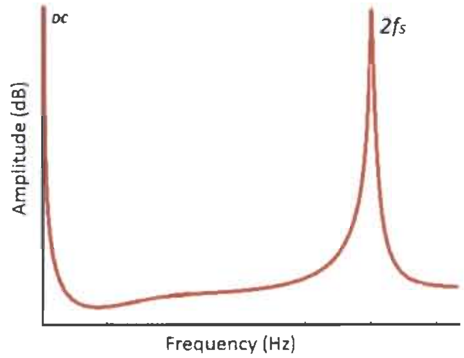

Figure 4.18: Stator Square Current Spectrum in normal operation mode

4.5.2 Broken Rotor Bar

in the case of broken rotor bars detection, the frequency spectrum is given by the next formula:

$$\begin{aligned} i_a^2(t) = &\left(\frac{I_{max}^2}{2} + \frac{I_{lsb}^2}{2} + \frac{I_{usb}^2}{2}\right) + \left(\frac{I_{max}^2}{2} + I_{lsb}I_{usb}\right) cos(2\omega t) \\ &+(I_{max}I_{lsb} + I_{max}I_{usb})cos(2s\omega t) + (I_{lsb}I_{usb})cos(4s\omega t) \\ &+(I_{max}I_{lsb})cos(2(1-s)\omega t) + (I_{max}I_{usb})cos(2(1-s)\omega t) \\ &+\frac{I_{lsb}^2}{2}cos(2(1-2s)\omega t) + \frac{I_{usb}^2}{2}cos(2(1-2s)\omega t) \end{aligned} \tag{4.26}$$

Once obtained the frequency spectrum 4.19, it is possible to detect a DC component, a $2f_s$ frequency component and sidebands on the frequencies $2(1 \pm 2s)f_s$. In addition, the spectrum presents components at frequencies $2sf_s$, $4sf_s$, $2(1-s)f_s$ and $2(1+2s)f_s$. These new components allow an early detection of broken or cracked rotor bars [28].

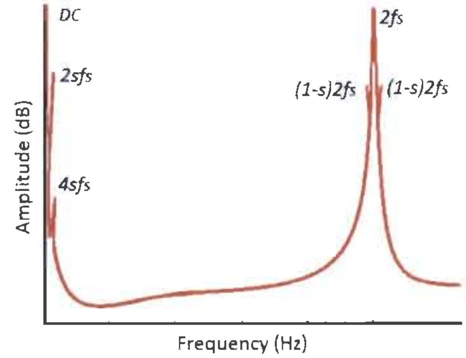

Figure 4.19: Stator Square Current Spectrum with Broken rotor bars

4.5.3 Eccentricity

For rotor eccentricity, the instantaneous square phase current is given by 4.27, highlighting new frequency components indicating the fault existence.

$$i_a^2(t) = \left(\frac{I_{max}^2}{2} + \frac{I_{lsb}^2}{2} + \frac{I_{usb}^2}{2}\right) + \left(\frac{I_{max}^2}{2} + I_{lsb}I_{usb}\right) cos(2\omega t) \tag{4.27}$$

$$+(I_{max}I_{lsb} + I_{max}I_{usb})cos(\omega_r t) + (I_{lsb}I_{usb})cos(2\omega_r t)$$

$$+(I_{max}I_{lsb})cos((2\omega - \omega_r)t) + (I_{max}I_{usb})cos((2\omega + \omega_r)t)$$

$$+\frac{I_{lsb}^2}{2}cos((2\omega - 2\omega_r)t) + \frac{I_{usb}^2}{2}cos((2\omega + 2\omega_r)t)$$

The spectrum in figure 4.20 shows a DC component, a frequency component $2f_s$, and sidebands at $2f_s \pm f_r$. But also additional components at f_r, $2f_r$ and $2f_s - 2f_r$. Thus, even for a motor with rotor eccentricity there are new frequency components that can be used for highlighting the detection of this type of fault [28].

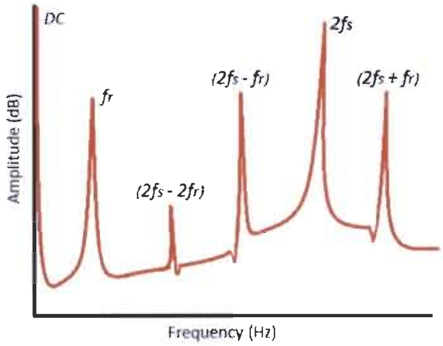

Figure 4.20: Stator Square Current Spectrum with rotor eccentricity

Chapter 5

Methodology and Experimentation

The methodology proposed for the project is described in 4 steps:

- System Construction and Learning

  a. Acquisition of the signals in normal operation mode and faulty mode. The signal required for the analysis is just the stator current in one phase of the motor, in order to know the behavior of the motor. In this part of the process, signals will be obtained through the support of National Instruments' data acquisition cards (DAQ) and the software of the same company LabVIEW ®.

  b. Pre-process the signal obtained with the use of mathematical techniques in order to improve the resolution of the obtained signal and reduce the presence of noise.
  To achieve this, techniques like Relative Harmonic Indexes (RHI) will also be required, in order to work in presence of noise, because this technique needs, a certain number of patterns in specific positions to make a proper detection.

  c. Generate the databases for both states (faulty and healthy state) that will be used later to compare the signals with the other obtained in the continuous monitoring. The database that will be generated, will be made mainly for three classifications:

  * **Healthy State:** represents the function of the motor in the normal operation mode, this means that the motor is working under the parameters specified by the manufacturer, (Typically 10% of under and over load).
  * **Faulty State:** For this case, the classifier will have two types of faults. The system will identify between, electrical and mechanical faults, and also different types of severity (low severity and high severity)
    Electrical faults are refer as faults on the rotor of the motor, more specifically broken rotor bars. Mechanical faults are refer as eccentricity on the shaft of the motor (dynamic eccentricity, static eccentricity and mixed eccentricity).

d. Introduce the data obtained into the classifier in order to train the technique. The classifiers proposed to develop in the project are: a)Fuzzy logic systems and b)Neural Networks, and the input variables are, the frequency and the amplitude of the signal obtained after the pre-process of the current.

e. Confirm the performance of the train, if it was successful go to step 6, if it was not successful pass to step 1 and repeat the process.

– Constant Motor Monitoring

  a. Start the continuous monitoring to obtain the current signal of the motor. In the same way that in the first step, DAQ will be connected in one phase of the motor connection, and the signal is going to be obtained on-line. It is worth to be mentioned, that the speed of the response of the program, (including the acquisition, the pre-process and the classification), depends totally on the capacity of the system and the specifications of the hardware.

– Fault Detection

  a. Pre-process the signal obtained with the use of mathematical techniques,(like Relative Harmonic Indexes, that have mentioned before on step 2), in order to improve the resolution of the signal obtained and reduce the presence of noise.

  b. Introduce the data obtained into the classifier and identify if there is a fault presented, if the system detect a fault go to step 9, if the system does not detect a fault pass to step 6 and repeat the process.

- Fault Diagnosis

  a. Classify the type of the fault and severity, depending on the amplitude of the harmonic.

     Once detected the failure in the motor, the system will conduct two activities:

     * The first one, is to diagnose the type of failure that is presented, this means, identify if the fault is electrical (broken rotor bars), or if the fault is mechanical (eccentricities).
     * The second part of the detection, is to determine the severity of the fault.

       If the fault has a low severity, the system will send an alert indicating that fault is presented, but also, a message that shows which are some possibles reasons of the fault, and how, the machine manager can correct it.

       If the fault has a high severity, the machine is going to stop instantaneously, (in order to prevent a disaster) and in the same way that in low severity, the system will send a message indicating the possible reason of the fault, and how to correct it.

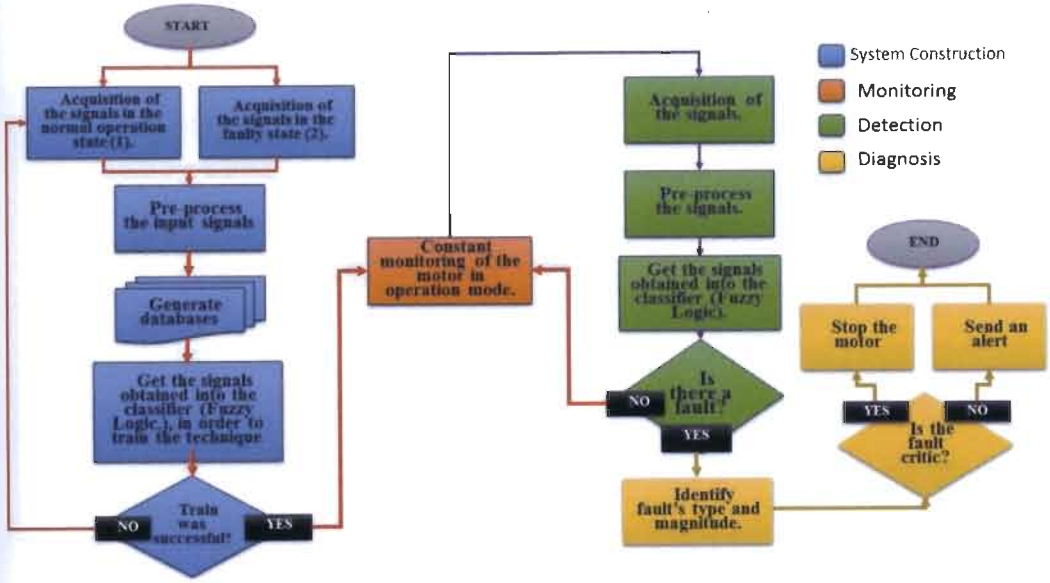

Figure 5.1: Methodology Diagram

In summary the process works as follows:
By the acquisition of the data, a current signal will be obtained, this signal will be represented by a vector magnitude "nx1", where "n" is equal to the number of observations Then, a pre-process will be made to the vector obtained (by using fast Fourier transform) with the objective of obtaining the variables that would indicate the presence of the fault (amplitude and frequency), that will be represented as an array of magnitude "nx2" where the first column represents the value of the amplitude of the harmonic, and the second column represents the frequency at where the harmonic is located.
Once these values are obtained, the matrix of "nx2" will be introduced into the classifier system (fuzzy logic) in which the classification will be performed, based on the stipulated rules.

The fuzzy system to be used will be a multiple input - multiple output. the inputs of the system will be:

- Amplitude

$$A = A_{ref} - Aactual \tag{5.1}$$

- Frequency

$$F \tag{5.2}$$

Some Fuzzy relations:

- IF the Frequency is "E.left" AND the Severity is "Low" THEN the output will be: "Broken Rotor" Bar with "Low severity"

- IF the Frequency is "M.Right" AND the Severity is "High" THEN the output will be:"Mixed eccentricity" with "High severity"

- IF the Frequency is "M.Left" AND the Severity is "Health" THEN the output will be:"Normal Operation Mode"

And the outputs will be:

- Type of fault
  * Electric Fault

$$\mu_{F_{E.left}} = \begin{cases} \frac{(F-(1-1.1s)2f_s)}{(0.1)f_s} & if \quad (1-1.1s)2f_s \leq F \leq (1-s)2f_s \\ \frac{(1-0.9s)2f_s-F}{(0.1)f_s} & if \quad (1-s)2f_s < F \leq (1-0.9s)2f_s \end{cases} \tag{5.3}$$

$$\mu_{F_{E.right}} = \begin{cases} \frac{(F-(1+0.9s)2f_s)}{(0.1)f_s} & if \quad (1+0.9s)2f_s \leq F \leq (1+s)2f_s \\ \frac{(1+1.1s)2f_s-F}{(0.1)f_s} & if \quad (1+s)2f_s < F \leq (1+1.1s)2f_s \end{cases} \tag{5.4}$$

  * Mechanical Fault

$$\mu_{F_{M.left}} = \begin{cases} \frac{F-0.9(2f_s-f_r)}{0.1(2f_s-f_r)} & if \quad 0.9(2f_s-f_r) \leq F \leq (2f_s-f_r) \\ \frac{1.1(2f_s-f_r)-F}{0.1(2f_s-f_r)} & if \quad (2f_s-f_r) < F \leq 1.1(2f_s-f_r) \end{cases} \tag{5.5}$$

$$\mu_{F_{M.right}} = \begin{cases} \frac{F-0.9(2f_s+f_r)}{0.1(2f_s+f_r)} & if \quad 0.9(2f_s+f_r) \leq F \leq (2f_s+f_r) \\ \frac{1.1(2f_s+f_r)-F}{0.1(2f_s+f_r)} & if \quad (2f_s+f_r) < F \leq 1.1(2f_s+f_r) \end{cases} \tag{5.6}$$

- Severity of the Fault
  * Normal Operation Mode

$$\mu_{A_{health}} = \begin{cases} \frac{A}{10} & if \quad 0 \leq A \leq 10 \\ \frac{15-A}{5} & if \quad 10 \leq A \leq 15 \end{cases} \tag{5.7}$$

  * Low Severity

$$\mu_{A_{low}} = \begin{cases} \frac{A-15}{5} & if \quad 15 \leq A \leq 20 \\ \frac{25-A}{5} & if \quad 20 < A \leq 25 \end{cases} \tag{5.8}$$

  * High Severity

$$\mu_{A_{high}} = \begin{cases} \frac{A-25}{5} & if \quad 25 \leq A \leq 30 \\ \frac{35-A}{5} & if \quad 30 < A \leq 35 \end{cases} \tag{5.9}$$

Finally, based on the values obtained at the outputs of the Fuzzy systems will be possible to determine which activity should be performed:

- Allow the motor to continue running if it is under normal operation mode.
- Report that there is a fault present and send the message with the corresponding correction if the severity of fault is low.
- Stop the motor and send the message with the corresponding correction if the severity of fault is high.

For this project, the work was carried about the detection of faults in electric motors by analyzing the current of one of the motor phases for its further analysis. Experimentation consisted basically in two steps, the first was the simulation of faults with the use of Multisim™ software. The second consisted in the performance of proofs directly to 2 motors installed on the workbench for test of analysis and fault detection. The tests developed are next described:

1. Eccentricity.
2. Broken rotor bars.
3. Voltage Unbalance.

The first step of the experimentation consisted on the simulation of the motor current, on two different behaviours; Normal operation mode, and Faulty mode with different levels of severity. The simulation were realized on a digital software (Multisim™) which emulates the performance of an electric circuit, in order to obtain a similar performance of an AC motor.
First, motor current was obtained in normal operation mode, for two different charge levels (full load and half load), then the motor current was obtained for faulty mode in two different scenarios, low severity and high severity.
To emulate the faults it was developed a system based on a motor's star connection as shown in figure 5.2. In the connection were established shortcircuits between the resistors in one phase of the motor, these shortcircuits generate an unbalance or fluctuations on the stator current which represents or emulate the behavior of an induction motor with broken rotor bars. The levels of fault were delimited by the connection of the resistors as are explained on table 5.

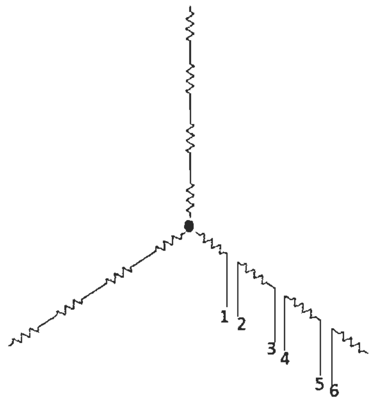

Figure 5.2: Stator Supply connection

Table 5.1: Connection table

Motor State	Level of Severity	Resistors Connections
healthy	0	1-2, 3-4, 5-6
Low severity	5%	1-2-3-4, 5-6
High severity	10%	1-2-5-6, 3-4

Once the signal is obtained, is proceed to perform some processing for the purpose of obtain patterns that would indicate the existence of faults, (in this case, specifically broken rotor bar).

5.1 Experimental setup

5.1.1 Work bench

Once, having tested the technique by simulation, it was proceeded to validate the technique directly to the squirrel cage induction motors located at the laboratory of analysis and fault detection provided by COMIMSA (Corporación Mexicana de Investigación en Materiales S.A. de C.V.).

The workbench for analysis and fault detection tests consists of 4 main parts:

- Two squirrel cage induction motors, 1 and 3hp, respectively (specifications on table 6.2) where the faults can be induced.
- Data acquisition system, composed by current sensors (ACS712) and a data acquisition card (DAQ) (specifications on table 6.3).
- Load simulation system (developed specifically for this project by the working group)
- Interface for data manipulation and processing.

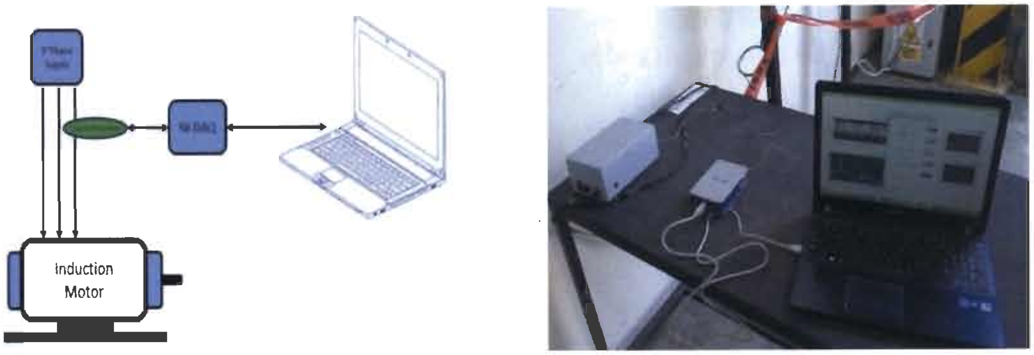

Figure 5.3: a)Connection Diagram b)Data acquisition system

Table 5.2: Motor specifications

Power	1 hp/0.75 kW	3 hp/2.24 kW
No. Poles	6	6
Voltage	230 V	230 V
Supply Frequency	60 Hz	60 Hz
Torque	4.56 lb-ft	13.41 lb-ft
RPM	1200	1200

Table 5.3: Data acquisition system specifications

Data acqusition card	NI-9201
single-ended channels	8
sample rate	500 kS/s
measurement range	$\pm 10V$
resolution	12-bit

Tests were developed for 3 specific faults: eccentricity, broken rotor bars and voltage unbalance; and for each fault, two different levels of severity: low severity and high severity.

In order to perform a successful implementation, some elements were required to simulate the faults and their different load levels. Those elements are next described.

For eccentricity fault simulation:

- 2 motor bushing of 0.75 and 1.375 inches of diameter respectively, to couple the slotted discs.
- 2 slotted discs (specifications on Table 6.4) used to attach the counterweights.
- Different counterweights to simulate the level of eccentricity.

For the proper implementation, the bushings required a machining, more specifically, a drilled on the external face for an oppressor's installation with the objective of adjust the bushing to the shaft.
The discs has 2 slots at the ends in which different weights are installed with the purpose of generate an unbalance on the rotor, similar behavior presented by an eccentricity fault. In the same way as the bushings, slotted discs were designed and manufactured.

Table 5.4: Slotted Discs specifications

Diameter	6 in	8 in
Drill Diameter	0.6 in	0.6 in
Distance from the center to the external slots	2.20 in	3.7 in
Distance between slots	4.4 in	7.5 in

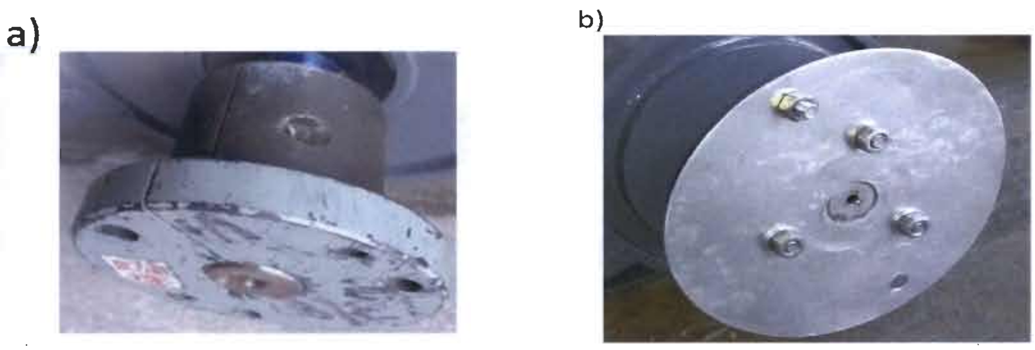

Figure 5.4: a)Bushing oppressor b) Slotted Disc

For load simulation:

- A calliper, used to brake the disc and simulate different level of load
- A brake pump; it was required to control the aperture level of the calliper.

These elements were installed at the end of the disc, in order to break the disc and thus to simulate different loads applied to the motor. 5.5

Figure 5.5: Load simulation system

For voltage unbalance, three power resistors were necessary, two of 1kW and 10 ohms each one and other of 1kW and 5 ohms. Resistors were installed in one phase of the motor (as seen on figure 5.6) with the purpose of generate different levels of voltage unbalance in order to known the behavior of the motor on these conditions.

Figure 5.6: Power resistors installation

For broken rotor bars, no way to simulate faults without damaging the motor was found. Based it was decided to make one and two drills on the rotor in order to broke

1 and 2 rotor bars, depending on the severity level of the fault, respectively (Figure 5.7).

Figure 5.7: Broken rotor bar

5.1.2 Data processing interface

The interface for processing and manipulation of data, was developed as follows in 4 principal phases:

- Acquisition phase: The current of one of the motor phases is acquired with the use of a current sensor (ACS 712) and a Data Acquisition Card of National Instruments^{TM} (NI-9102) for further processing. It is worth to be mentioned that a sampling rate of 100 ks was used for data acquisition, as well as a low-pass filter in order to reduce bad-functions in the signal
- Processing phase: This phase has two main steps; a)The processing of the signal in order to raise the current to square, with the objective of have better resolution. b)In order to obtain the patterns of the harmonics, it was transformed the current from time domain to frequency domain with the use of a spectrogram, used to detect the fault. (Both processes, data processing and transformation were realized with the use of LabVIEW^{TM} software.)

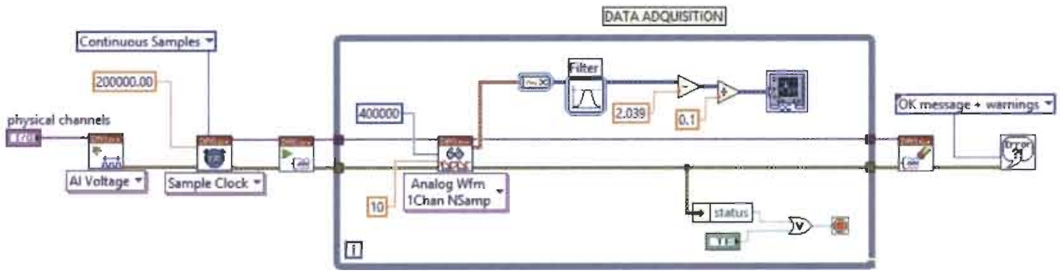

Figure 5.8: Connection diagram for data acquisition

The figure 5.8 presents the program developed for the data acquisition, the first block is used to determine the type of the variable to read, the second block is used to determine the acquisition speed (200 ks/s) and then the start block. Subsequently a loop was established to generate a constant reading; Inside the loop a block to read the signal obtained and other to visualize it in the front panel. Finally out of the loop, a block to reset the data collected to make a continuous acquisition system.

- Analysis phase: Once, having the signal in frequency domain, specific frequency harmonics were selected, identifying their location and amplitude to be used later in the detection phase.

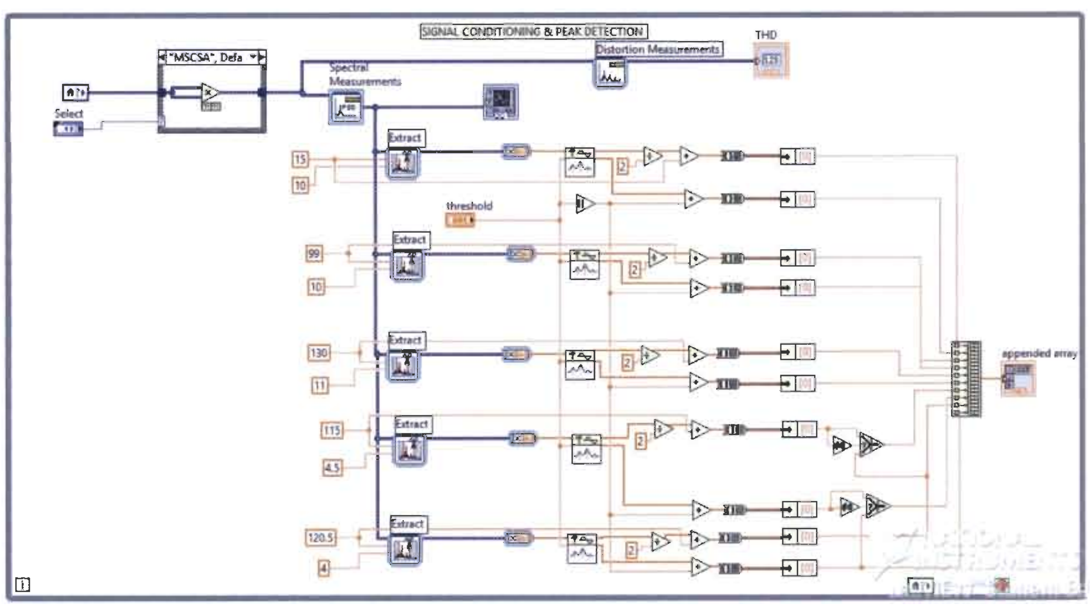

Figure 5.9: Connection diagram for data processing

Figure 5.9 presents the part of the program dedicated to transform the signal from time domain to frequency domain and consequently to select the harmonics for patterns recognition. The first block, located at the top left-hand corner is used to square the current. The blocks located at the center on the top are in charge to convert the signal to the frequency domain and then to display the graph to the front panel. Next blocks located in the center from the top to the bottom have the same purpose, the first block is used to select an specific part of the periodogram (depending in the range of the selected harmonics) and the next block is used to get the information about those harmonics (frequency and amplitude). Finally at right at center, all the variables selected are joined in to a single array as the input for the fuzzy system.

- Detection phase: In this part, the selected patterns (frequency and amplitude) were introduced in a Fuzzy system to detect the type and severity of the fault.

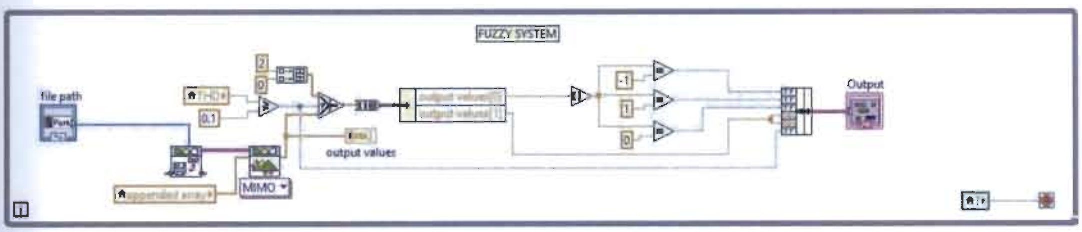

Figure 5.10: Connection diagram for fuzzy controller

The last part of the program (shown on figure 5.10) is dedicated to the detection and diagnosis of the fault with the use of a fuzzy system. The first two blocks are used to determine the fuzzy system saved on the computer. The next block shown on orange, is the array obtained on the processing part of the program and is introduced to the fuzzy system. In this case, the system used is a Multiple Input Multiple Output (MIMO). Finally on the right side of the loop, the outputs obtained from the fuzzy system (fault type and severity) are unbundle and displayed in a graphical way, represented as the leds and the progress bar shown on the front panel of the interface.

5.2 Eccentricity

The bushing and the slotted disc were installed to the shaft and 40 runs were executed with the aim to know the behavior of the motor on normal operation mode. Next, different counterweights were added in one of the slots of the disc in order to generate an unbalanced on the shaft, simulating an eccentricity fault (as it is show on Figure 5.11).

Figure 5.11: Eccentricity Fault simulation

To determine the counterweights required to generate different levels of fault severity, 120 proofs to each motor were carried out. After to determine the counterweights, 80 runs were developed to determine the weights and 40 to test them. Table (6.5) shows the counterweights.

Table 5.5: Counterweights definition

Operation mode	Counterweight	
	1 hp	3 hp
Normal	0 grs.	0 grs.
Low severity Fault	50 grs.	200 grs.
High severity Fault	100 grs.	400 grs.

To signal analysis, 2 methodologies were used, MCSA and MSCSA, in order to show the advantages of working with the square current.

Once obtained the current signal and having preprocessed it with the use of a spectrogram, it was started with the analysis, which basically consists of two steps. The first is a visual analysis directly to the graph aiming to identify highlighting harmonics. The second one is to make a numerical analysis of those harmonics, gathering precise information about the frequency and amplitude of the selected harmonics.

5.3 Voltage Unbalance

One of the objectives of the project, was to developed a system to detect different types of fault (eccentricity and broken rotor bars), but also to create a system able to work with noise presence, more specifically, electrical noise.
Therefore, the aim of this part of the project, was to determine a new pattern that could give information about the quality of the supply current, in order to differentiate between a fault occasioned by a problem on the electrical current, or a fault directly in one of the principal motor parts.

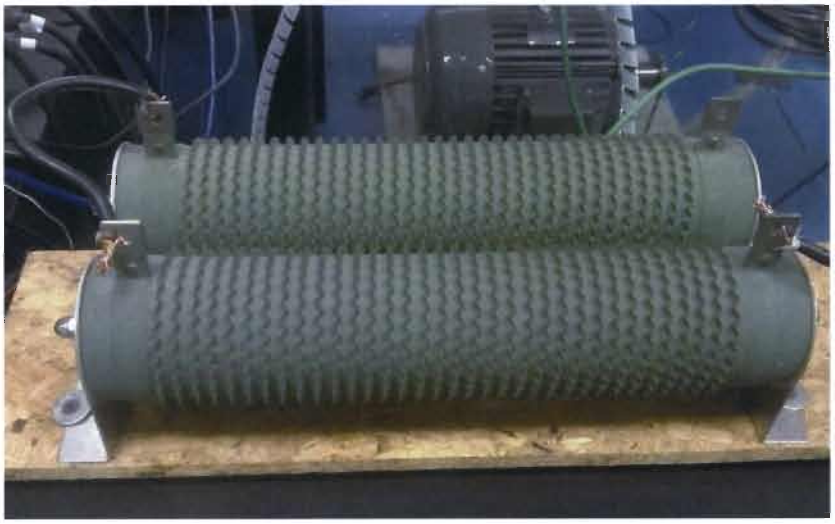

Figure 5.12: 10 ohms 1kW power resistors

One of the existing techniques used to identify the quality of the supply current, is THD (Total Harmonic Distortion) which is defined as the relative signal energy present at non-fundamental frequencies. [33].
Harmonic distortion occurs when the output signal of a system is not equal to the input signal, frequently affected by the presence of different devices on the same network,

generating distortion on the signal (multiples of the supply current) that can cause problems on the performance of the electrical equipment.

To validate the efficiency of the technique, several tests were developed. They consisted on the installation of different power resistors in one of the phases of the motor to generate a different voltage according to the other two phases in order to cause a voltage unbalance on the motor, that represent a bad quality on the current.
Subsequently, the generated signal was analyzed with the spectrogram to determine the Total Harmonic Distortion of the current to collect information about the motor behavior under these conditions.

This part of the project consists basically into two steps. The first, was to analyze the current on normal operation mode without voltage unbalance. However, with the purpose of provide a tolerance range to the system, getting the possibility of work in presence of noise, tests with certain unbalance were developed.

The second step of the project was to analize the current under faulty conditions. In this case, faulty conditions were constituted by 2 levels of fault: low and high unbalance voltage. The specifications of these unbalances are next described.

Table 5.6: Voltage Unbalance Specifications

Fault level	Power resistor	Voltage Unbalance	THD
Normal Operation	0-5 Ω	0-7 Vac	0-3 %
Low severity	10 Ω	20 Vac	7-9 %
High severity	20 Ω	32 Vac	19-21 %

5.4 Broken Rotor Bars

The simulation of broken rotor bars consisted basically on three steps: monitoring and diagnosis of the motor current in normal operation mode, monitoring and diagnosis of the current with one broken bar and with with two broken bars. It is worth to be mentioned, that for each operation state, 2 different load conditions were required, low load condition and high load condition.
In Figure 5.13 is shown the rotor without used to tests, without damage, representing the normal operation mode.

Figure 5.13: Rotor without damage

Subsequently, it was proceeded to perform tests under faulty mode, in low severity (one broken bar) and high severity (two broken bars).
To induce this fault, it was necessary to drill holes in the external face of the rotor. In case of low severity, one hole was necessary and in case of high severity, two holes were required. It should be noted that for each level of fault, different load conditions were required. In case of low load level, the slip was established in the range 0.0083 - 0.0125 and in case of high load condition, the slip varies from 0.0208 to 0.029.

a) b)

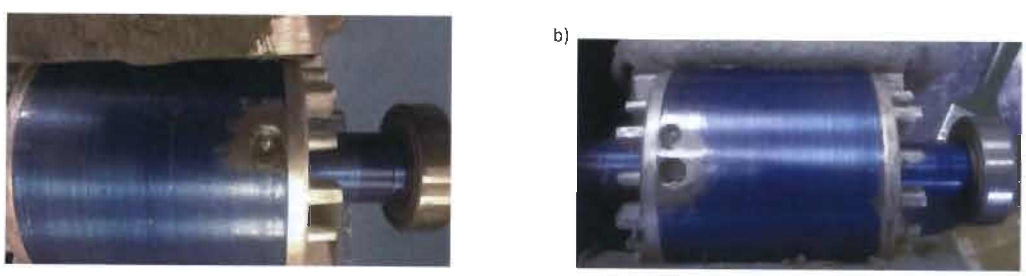

Figure 5.14: Damage rotor a)One broken bar b)Two broken bars

Chapter 6

Results and Discussion

6.1 Results

The first part of the experimentation was the Fault simulation via software, results obtained are next explained:

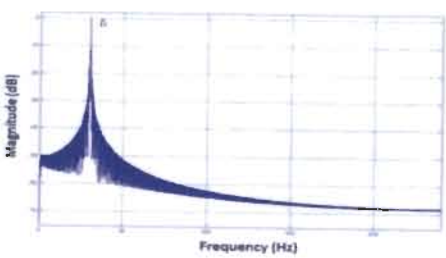

Figure 6.1: MCSA healthy state

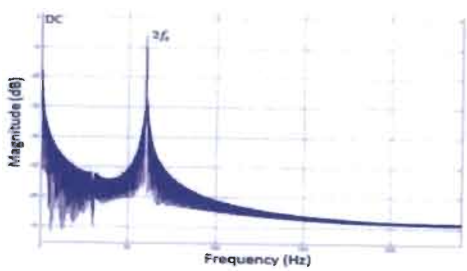

Figure 6.2: MSCSA healthy state

Figures 6.1 and 6.2 shown results for the signal obtained on normal operation mode, where it can be observed just the patterns f_s for MCSA and for MSCSA a DC pattern and the fundamental frequency on $2f_s$.

On the next figures are presented result for both techniques in faulty state, with a low level of severity. In the figure 6.3 can be observed that MCSA present patterns in the frequencies $(1-2s)f_s$ and $(1+2s)f_s$ that indicates the presence of broken rotor bars in the motor.

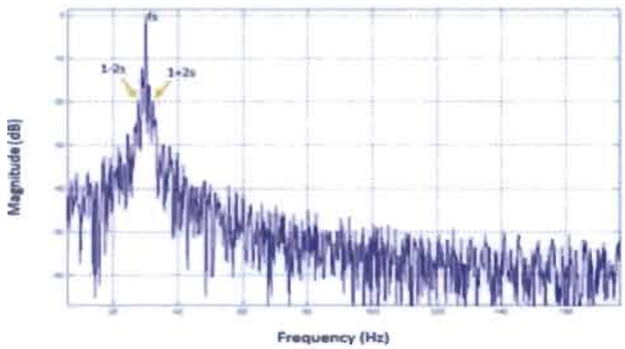

Figure 6.3: MCSA high severity fault

In the case of MSCSA the frequency spectrum shows patterns on the frequencies $(1 \pm 2s)2f_s$ but also on the frequencies $(1 \pm 4s)2f_s$ and $(1 \pm 6s)2f_s$, which represents a little advantage over MCSA because it has greater detection features. Figure (6.4)

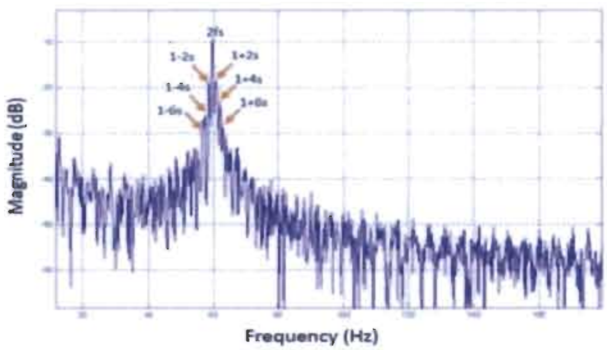

Figure 6.4: MSCSA high severity fault

But, the greatest advantage that presents MSCSA over MCSA is presented when the motor is under low load conditions, because MCSA is not able to detect patterns. In case of MSCSA it is possible to observe some patterns $(2f_s, 4f_s, 6f_s, 8f_s)$ that indicates the fault under these conditions. Figure (6.5)

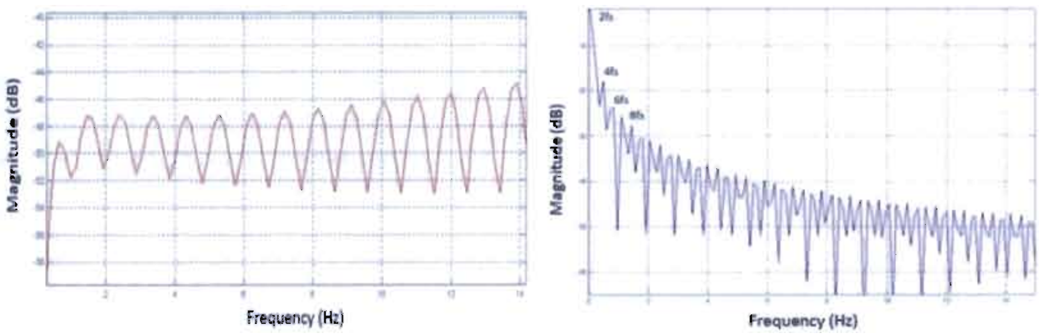

Figure 6.5: MSCSA low severity fault

6.1.1 Eccentricity

For eccentricity tests, results are next explained. On the first graphs, showed on Figure 6.6, can be observed the frequency spectrum of the normal operation mode for both motors(a)1hp b)3hp), which shows just one remarkable harmonic on the main frequency f_s

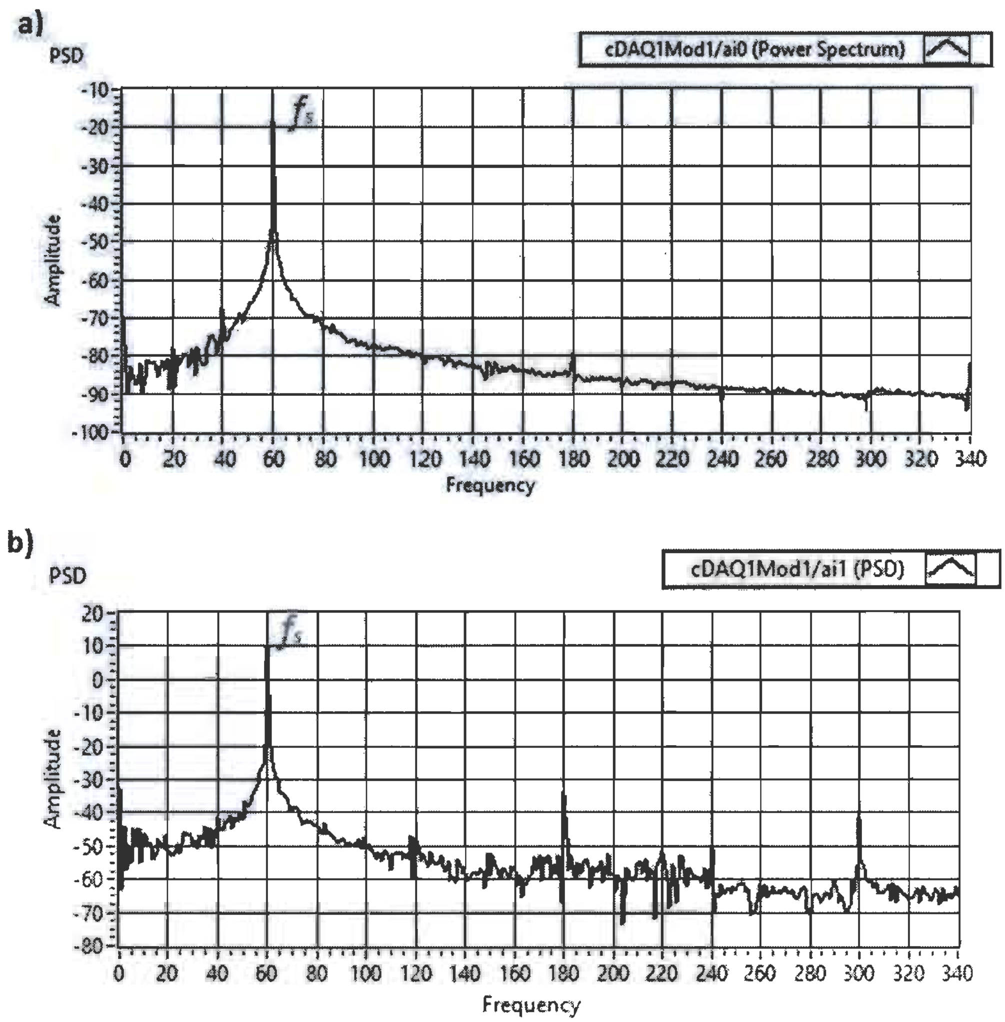

Figure 6.6: MCSA Frequency spectrum of Normal Operation Mode a)1hp b)3hp

The graph shown on figure 6.7 presents the frequency spectrum corresponding to the current analysis of the eccentricity fault at low severity. It is possible to see significant harmonics at frequencies $f_s \pm f_r$ warning about a bad function on the motor.

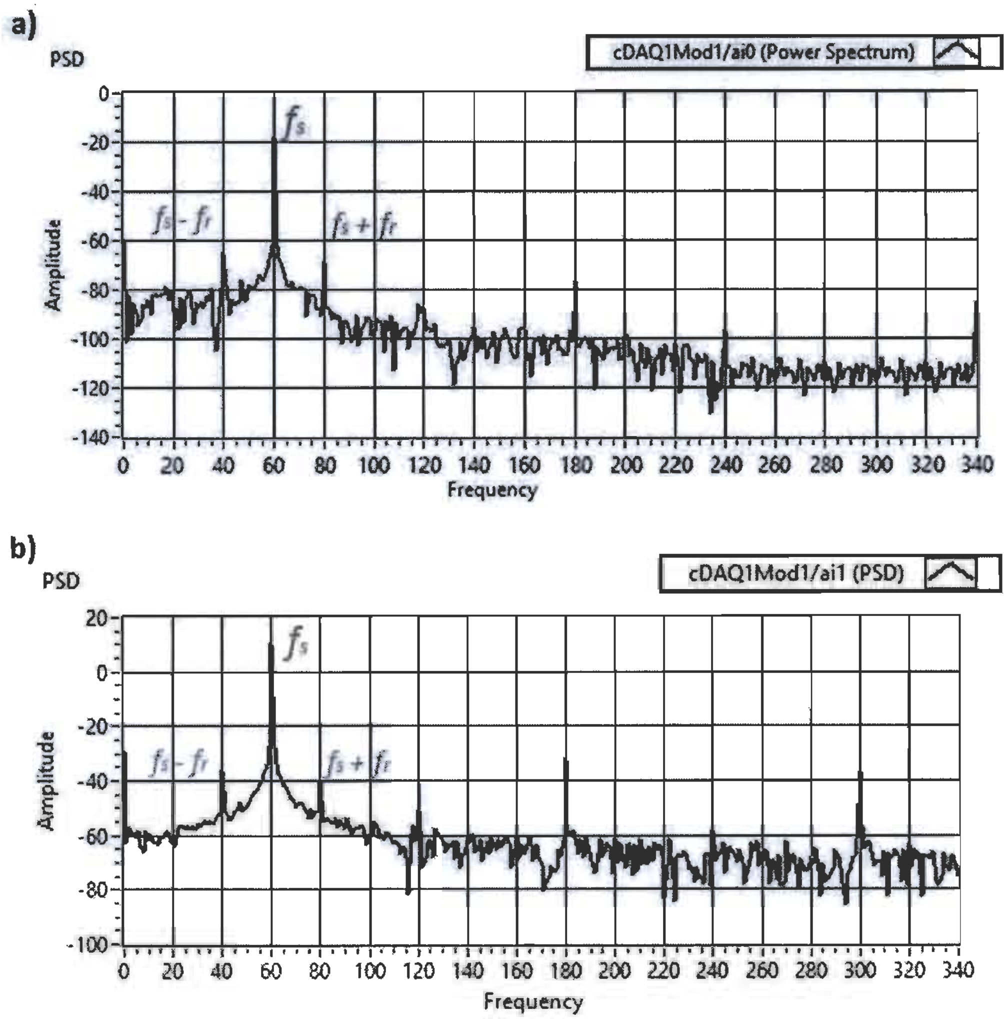

Figure 6.7: MCSA Frequency spectrum of eccentricity fault with low severity a)1hp b)3hp

Observing the figure 6.8, corresponding to the high severity fault. It is possible to see the amplitude increase on the selected harmonics when the unbalance is higher denoting the amplitude as the pattern used to detect the severity of the fault.

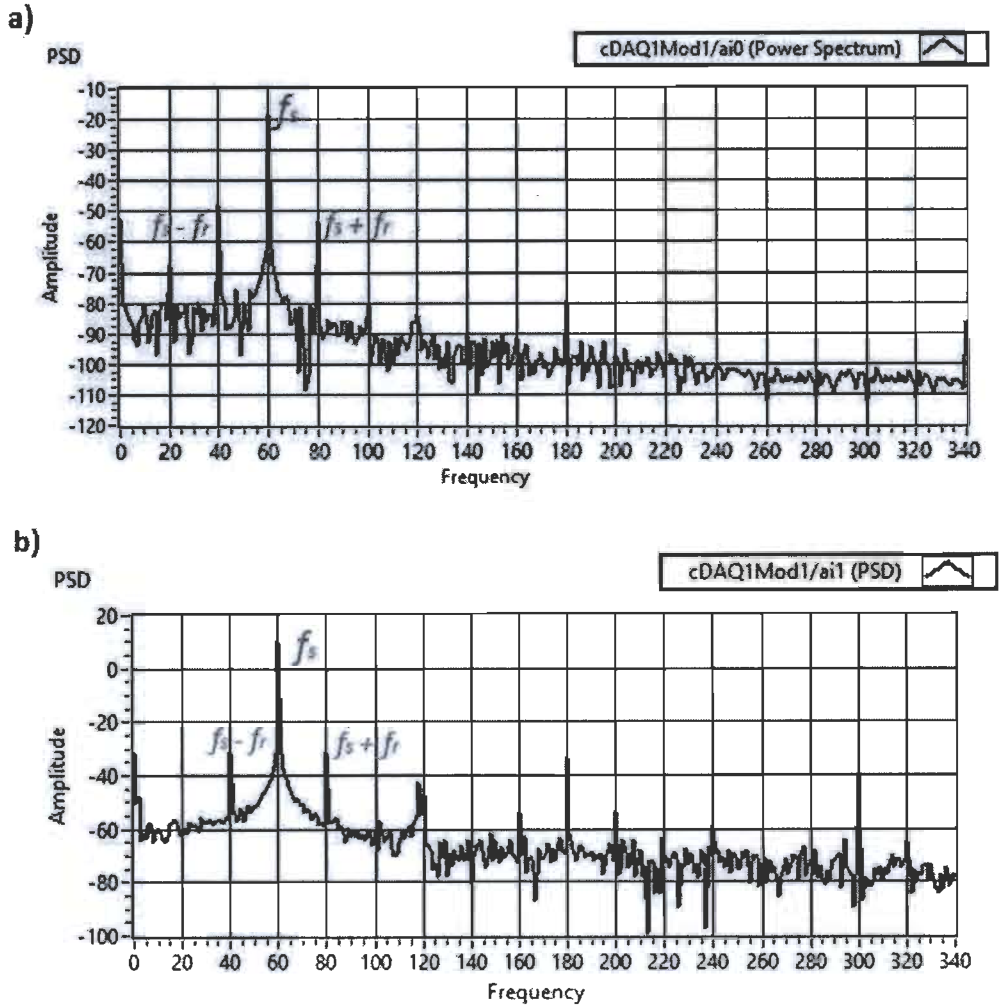

Figure 6.8: MCSA Frequency spectrum of eccentricity fault with high severity a)1hp b)3hp

Based on the results obtained, 3 principal frequencies were established as patterns to make a correct diagnosis. The rotor frequency f_r located at 20 Hz, rotor frequency less supply frequency $f_s - f_r$ located at 40 Hz, and rotor frequency plus supply frequency $f_s + f_r$ located at 80 Hz. The determined values are showed in Table 6.6.

Table 6.1: MCSA detection patterns for eccentricity

	Normal Operation	Low severity	High severity
Frequency	Amplitude		
20 Hz	0 dB	0-5 dB	5-10 dB
40 Hz	0-5 dB	5-15 dB	15-25 dB
80 Hz	0-5 dB	5-10 dB	10-20 dB

After the analysis with the current in normal operation, it was continued to perform the analysis with the square current, aiming to detect more patterns and also maximize the spectrogram resolution.

For this technique, it was necessary to preprocess the current signal, to raise it to square, and consecutively transform it from time domain, to frequency domain (both processes were developed on LabVIEW ® software).

In Figure 6.9 can be observed a simple harmonic on the supply frequency, at $2f_s$, indicating that the motor is working in normal operation mode.

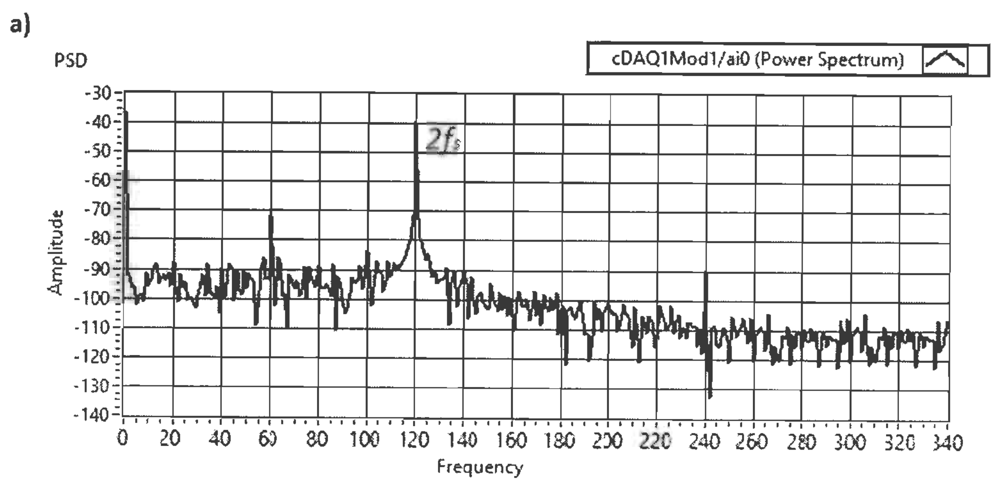

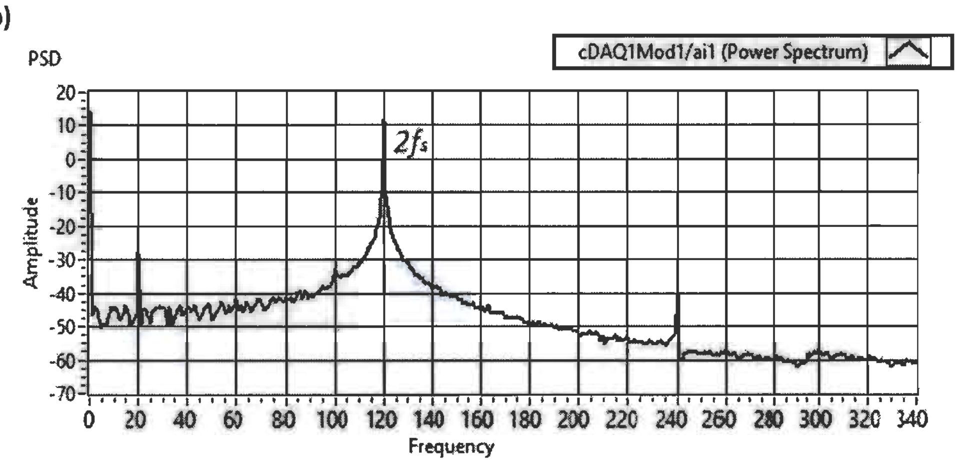

Figure 6.9: MSCSA Frequency spectrum of Normal Operation Mode a)1hp b)3hp

On the other hand, Figure 6.10 shows the spectrogram for a faulty state, more specifically, eccentricity on low severity level. It is possible to observe highlighting harmonics at the frequencies $2f_s - fr$ and $2f_s - fr$, and also the rotor frequency harmonic f_r, which refers to eccentricity fault.

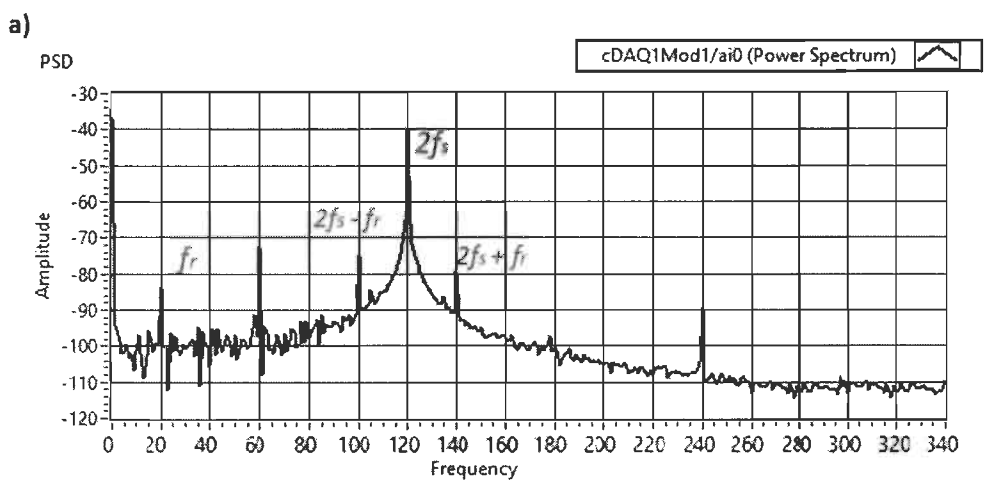

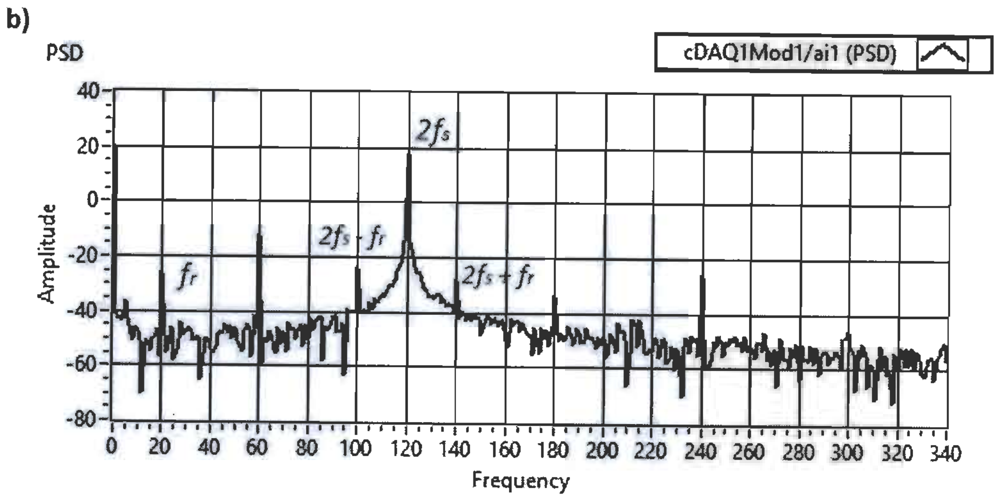

Figure 6.10: MSCSA Frequency spectrum of eccentricity fault with low severity a)1hp b)3hp

The advantage of this technique is presented when the severity level increases, because, besides of presenting a higher resolution speaking about the amplitude, additional harmonics are presented, which can be selected as new patterns in order to make a proper diagnosis of the fault.

In the figure 6.10 is shown the spectrogram of an eccentricity fault with high severity level, in which an additional harmonic can be observed at $2f_r$ frequency, and also the same harmonics at frequencies $2f_s \pm f_r$ and f_r respectively, but on different amplitude level.

a)

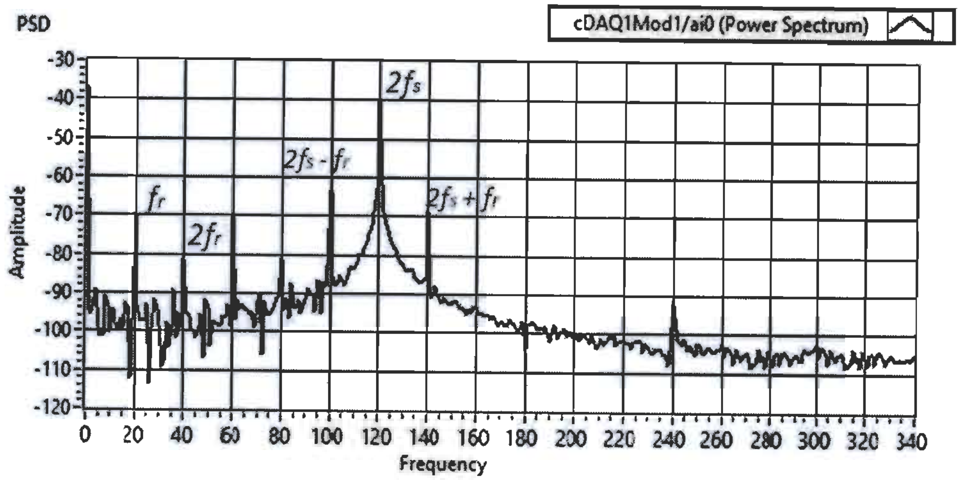

b)

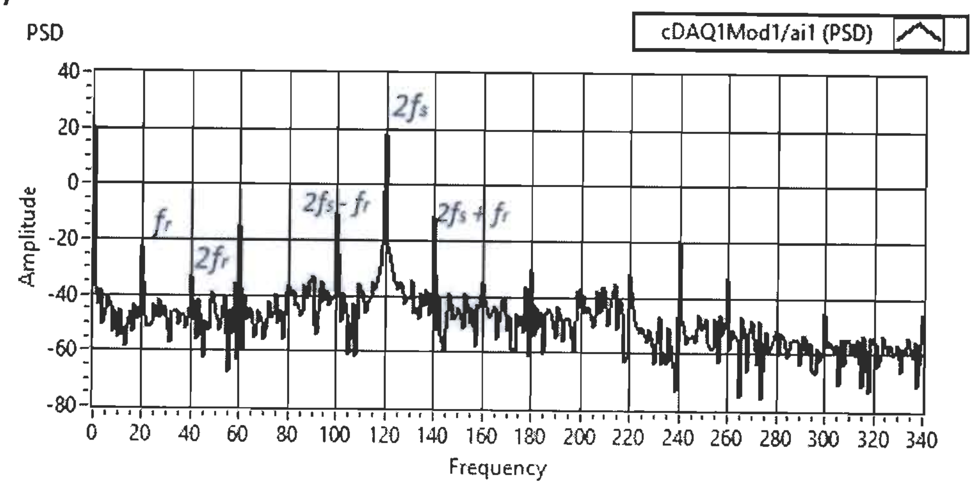

Figure 6.11: MSCSA Frequency spectrum of eccentricity fault with high severity a)1 hp b)3 hp

Based on this information, it was determined 4 main frequencies as patterns to detect and diagnose the fault. Rotor frequency (f_r)located at 20 Hz, twice rotor frequency ($2f_r$) located at 40 Hz, and twice supply frequency $\pm$ rotor frequency ($2f_s \pm f_r$)located at 100 Hz and 140 Hz respectively; Table 6.7 shows the amplitudes of the selected harmonics for different levels of severity.

Table 6.2: MSCSA detection patterns for eccentricity

	Normal Operation	Low severity	High severity
Frequency	Amplitude		
20 Hz	0-10 dB	10-20 dB	20-30 dB
40 Hz	0-5 dB	5-15 dB	15-25 dB
100 Hz	0-5 dB	10-20 dB	20-40 dB
140 Hz	0-5 dB	10-20 dB	20-35 dB

It is possible to detect the difference between the amplitude ranges in Tables 6.6 and 6.7 for each selected harmonic at different levels of fault, besides of the detection of a new harmonic. These new patterns show highly relevant results when detecting the type of fault and provide a more sensitive technique to determine the severity of the fault.

6.1.2 Voltage Unbalance

For this test was required the use of a 5 ohms power resistor which generate an unbalance of 7V for its further analysis. In the spectrogram showed on Figure 6.12 highlighting harmonics can be observed at frequencies 240, 360 and 480 Hz (multiples of the supply frequency). Nevertheless after the analysis of the THD (2.38 %)it is possible to determine that their amplitude has not big relevance.

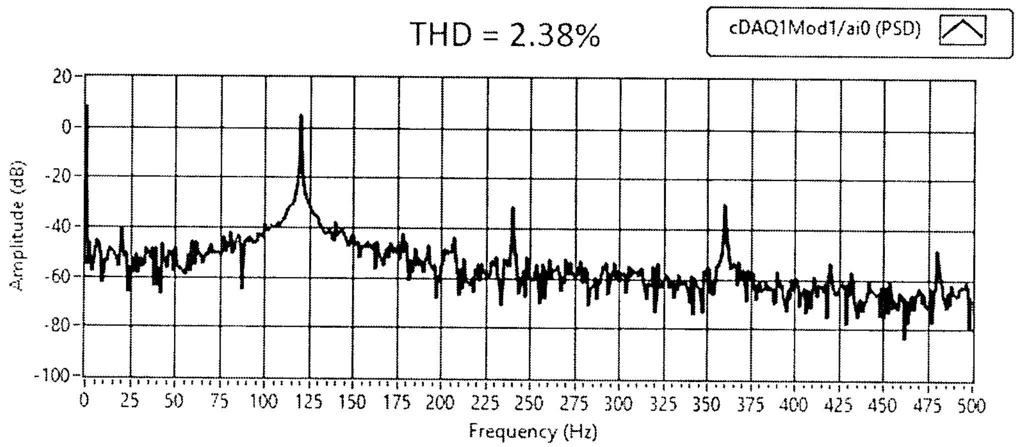

Figure 6.12: Frequency Spectrum and THD for Normal operation mode

After having determine the levels of unbalance in the voltage, it was proceeded to start with the tests. In the Figure 6.13 can be observed the spectrogram of the current with an unbalance of 20 Vac. This unbalance can be determined basically in two steps. First, in the graph is possible to see how the multiples harmonics of the supply frequency had increased considerably (10-15 dB approximately), that can be used as a first index that quality of the current it is inadequate. The second step consists to obtain the Total Harmonic Distortion of the current, and determine the range of values. In this case Figure "a" shows that THD is 8.65 % , corresponding to a low severity unbalance. Similarly, Figure "b" shows the frequency spectrum of the current with an unbalance of 32 Vac, which leads to a high severity unbalance causing a THD of 21.76 % and an increase of 15 to 25 dB on the selected harmonics.

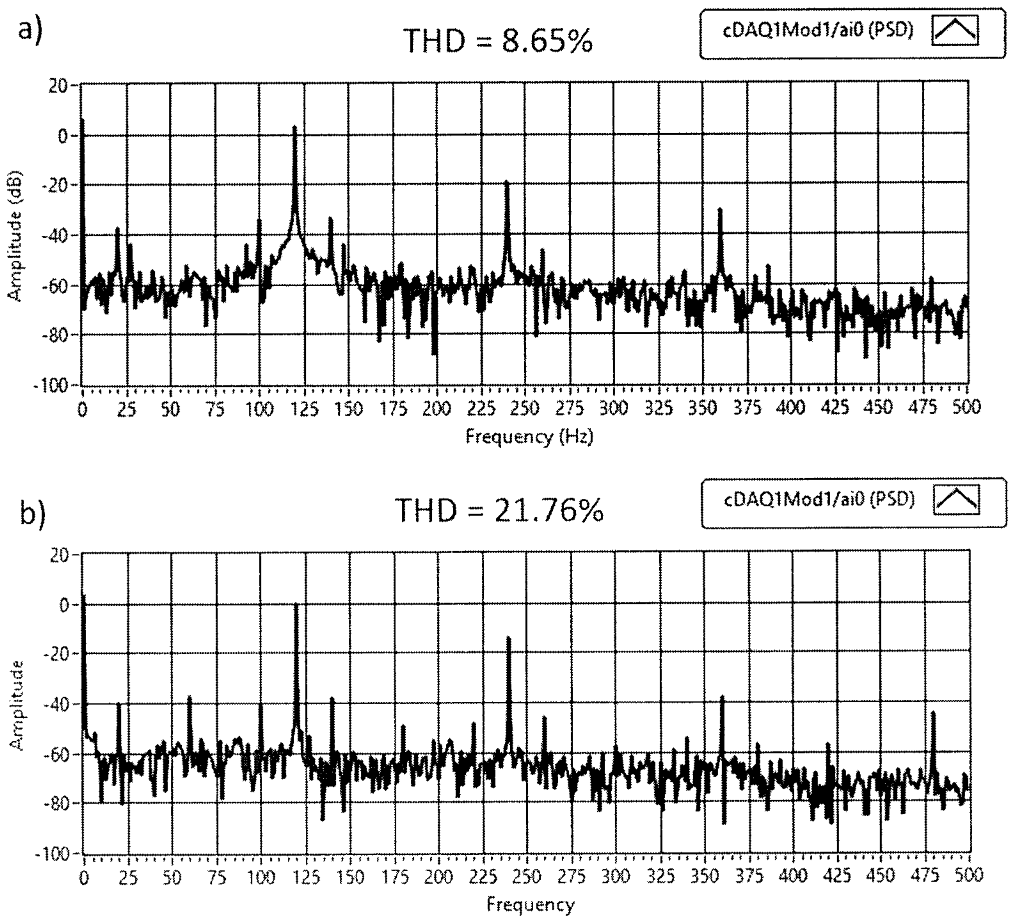

Figure 6.13: Spectrogram of Voltage unbalance a)Low severity b)High severity

Finally, several tests were developed to detect the THD in the presence of eccentricity broken rotor bars. The results obtained were THD = 2.5 - 4 % for eccentricity and THD = 4 - 6 % for broken rotor bars. Based on these information, the next relation was established. If the THD is less than 10 % the system continue with its normal function detecting broken rotor or eccentricity. On the other hand, if THD is equal or higher that 10 % , the problem would be caused by a voltage unbalance.

6.1.3 Broken Rotor Bars

The first part of this simulation consisted on the acquisition of the motor current in a state of normal operation for its further analysis through a frequency spectrum to analyze the motor current without damage on the rotor. The frequency spectrums obtained shows the supply frequency harmonic at $f_s = 60Hz$ in case of MCSA and $2f_s = 120Hz$ in case of MSCSA, indicating the correct function of the motor.

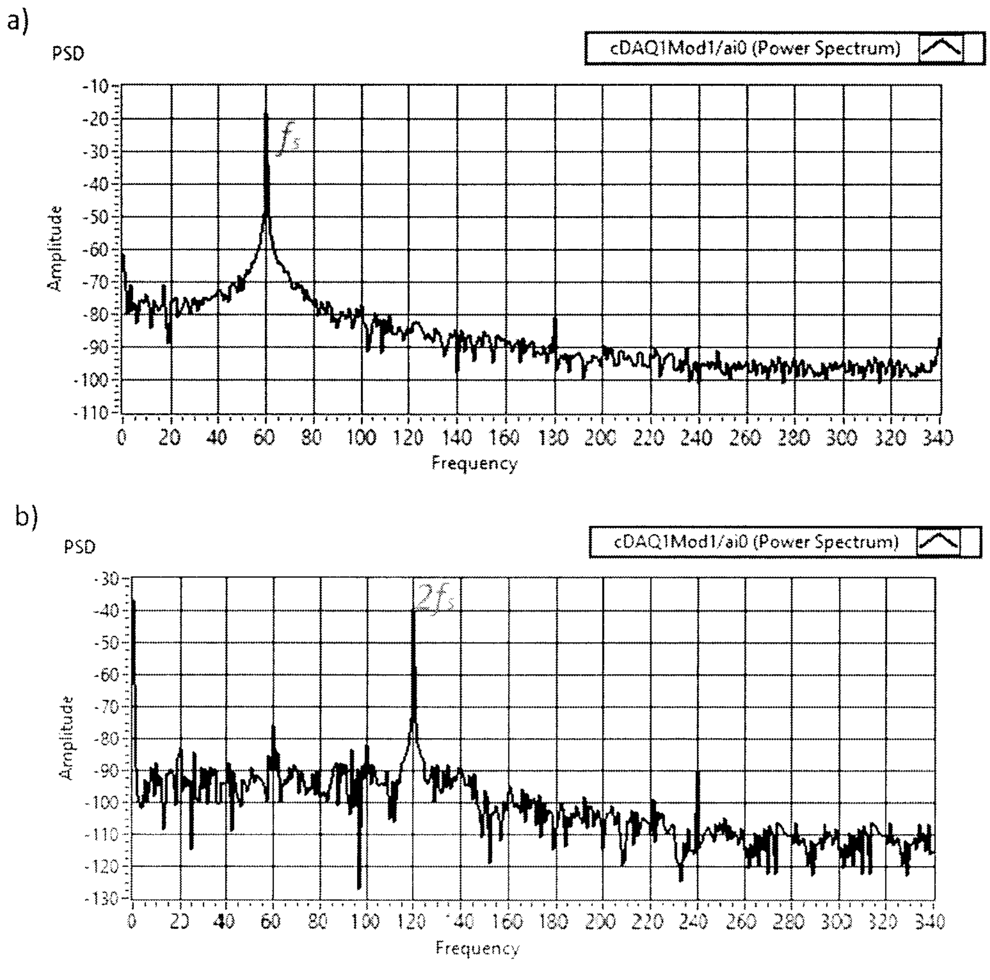

Figure 6.14: Frequency Spectrum Healthy State

In Figure 6.15 it is shown the frequency spectrum of the current obtained with one broken bar and low load. The graph "a" presents the spectrum using the technique MCSA, in which is possible to see two sidebands at frequencies $(1 \pm s)f_s = 40$ and

80 Hz, around the supply frequency $f_s = 60$ Hz. The graph on the right side, shows the spectrum in use of the technique MSCSA presenting highlighting harmonics at frequencies $(1 \pm s)f_s$. In this case, it can be observed other patterns at frequencies $(1 \pm 3s)f_s$, that indicates the presence of a broken rotor bar.

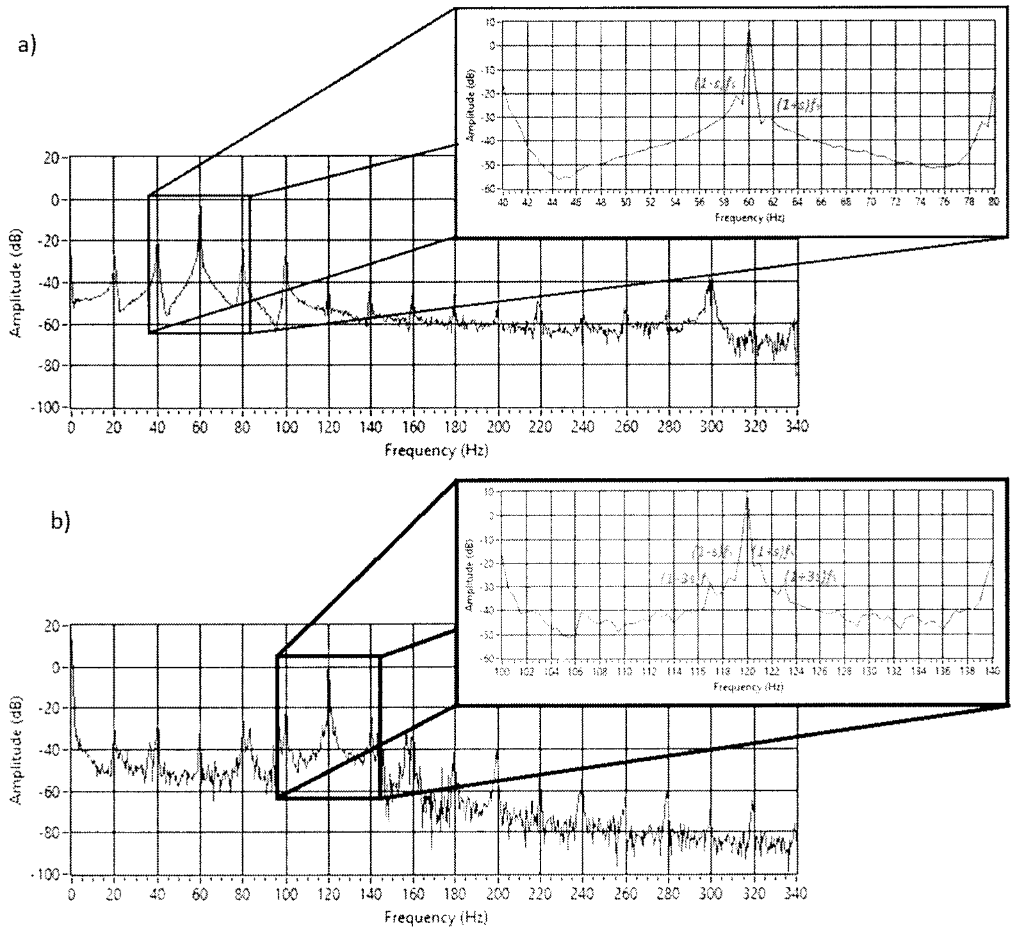

Figure 6.15: Spectrum of the motor current with one broken rotor bar and low load condition a)MCSA b)MSCSA

Next, Figure 6.16 shows the frequency spectrum of the current obtained with one broken bar under high load conditions. It can be observed sidebands patterns on both sides of the main frequency. Also it is possible to notice that as increase the load, the distance is greater between the sidebands and the supply frequency harmonic. This is because, when the load gets higher, the slip gets higher. The analysis gets a better resolution when the load is incremented. However, if the graphs shown are observed more closely , it is possible to notice the benefits to work with the square of the current. The resolution in terms of the number of harmonics is improved providing a greater number of patterns to use increasing the precision of the technique.

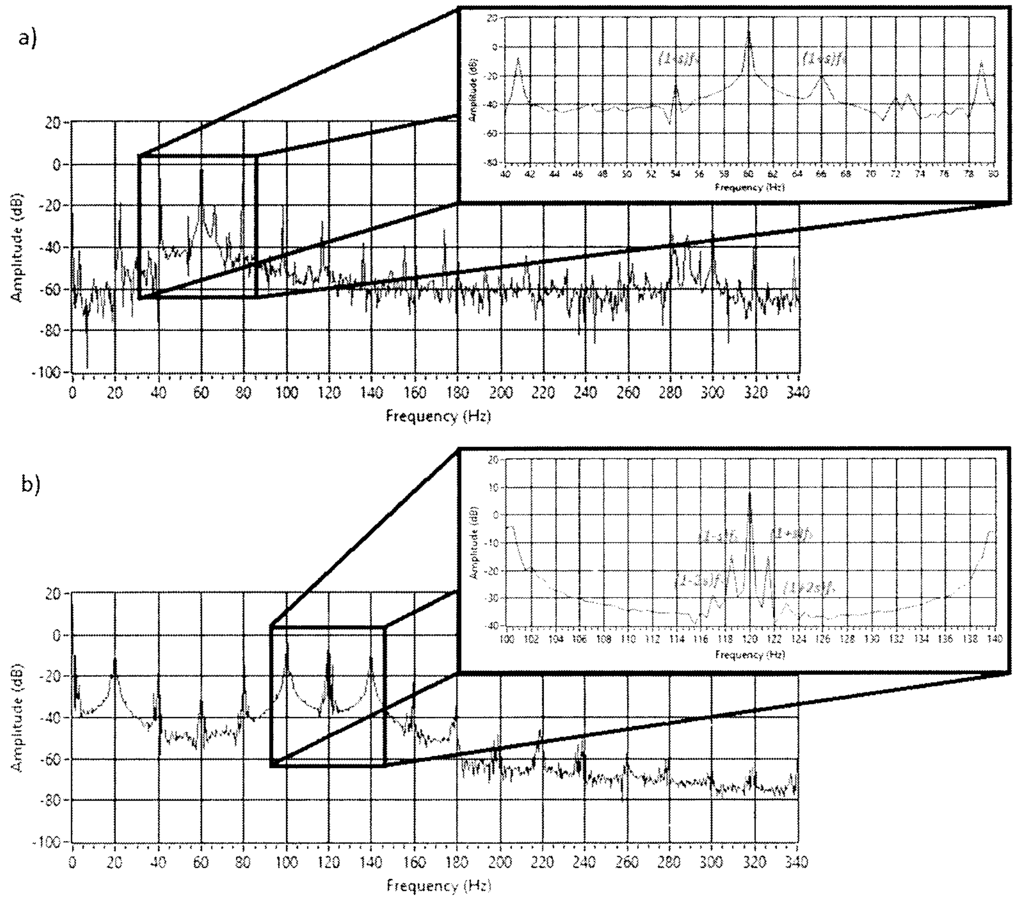

Figure 6.16: Spectrum of the motor current with one broken rotor bar and high load condition a)MCSA b)MSCSA

Once, having performed the tests with one broken bar, it was continued to test the system with 2 broken bars and also with two different load levels. The first graph 6.17, presents the analysis with the use of the technique MCSA in low load condition, in which is possible to see the harmonics $(1 \pm s)f_s$, and on the right side of the supply frequency an extra harmonic in the frequency $(1+2s)f_s$, that represents an increase in the number of patterns to make a better diagnosis. Nevertheless, if the MSCSA graph is analyzed closely can be observed an increase of the resolution in the number of detected patterns and the amplitude of this patterns represent a significantly difference between a fault with low severity (one broken bar) and a fault with high severity (two broken bars).

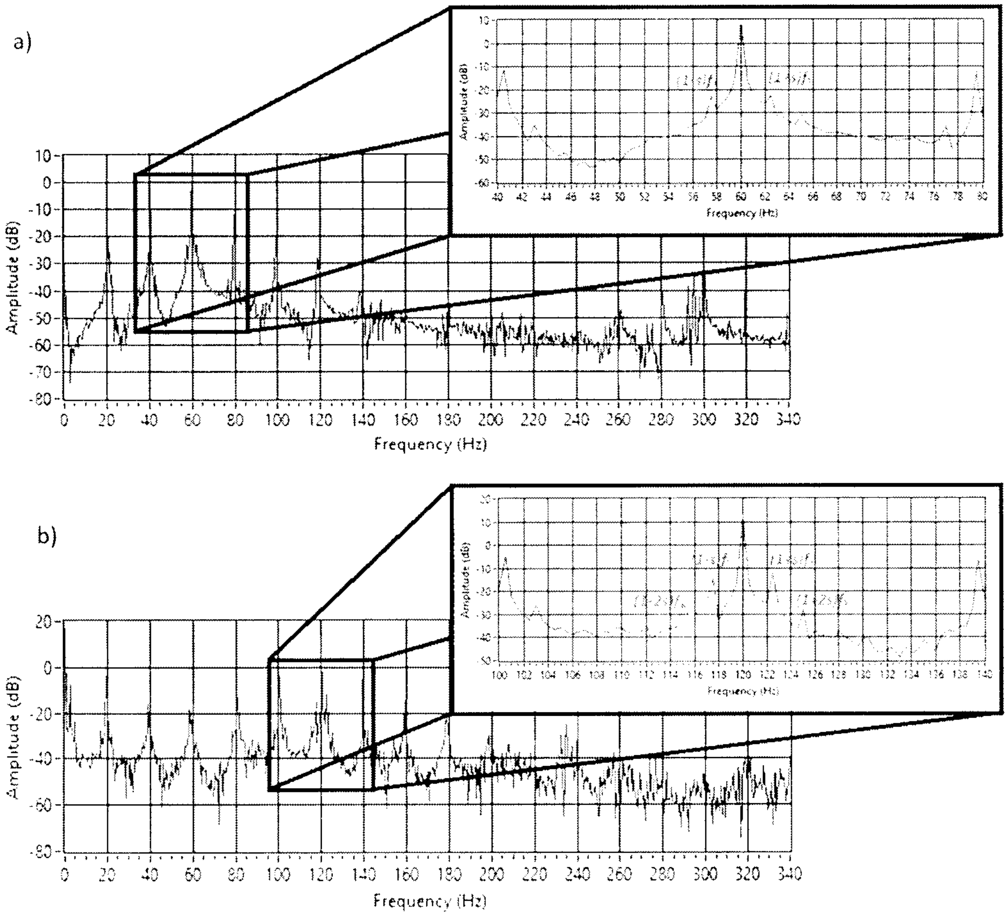

Figure 6.17: Spectrum of the motor current with two broken rotor bars and low load condition a)MCSA b)MSCSA

The load impact of the spectrogram was determined. For that, tests with two broken bars were performed, but now under high load conditions. The Figure 6.18, shows in part "a" the frequency spectrum of the technique MCSA, in which it is possible to see an increase on the distance between the supply frequency and the sidebands. In this case difference of the amplitude was not significant. On the other hand, if it is observed the graph "b" by the use of the technique MSCSA, it is easy to detect some differences. For example, the number of patterns increase from 4 to 6, adding two extras harmonics at frequencies $(1 \pm 3s)f_s$. Another advantage detected is the amplitude presented on the sidebands, which are almost the double of the presented on the previous analysis. These differences represent a great advantage to make a correct diagnosis. Having a greater number of patterns, make it easier to determine more precisely if the fault is occasioned by an eccentricity or a broken rotor bar. Moreover, talking about the severity of the fault, the necessary tools can be provided to the user to differentiate between a proper maintenance on time or total motor fault.

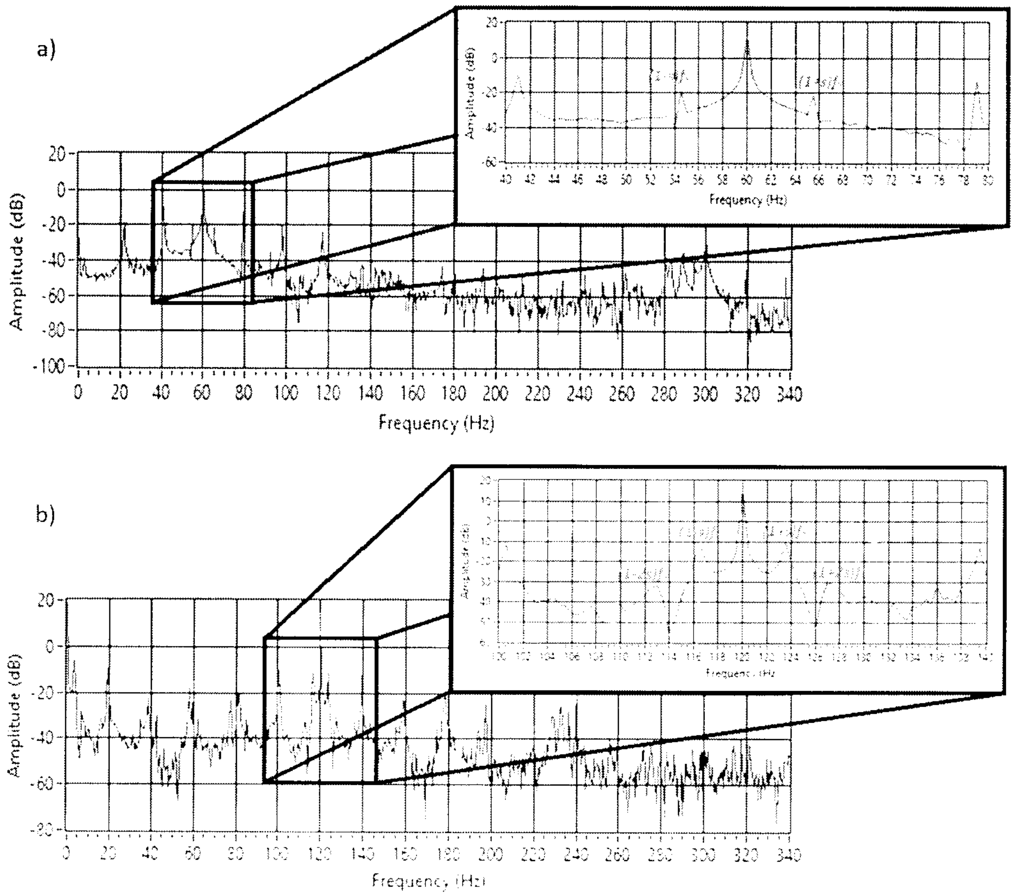

Figure 6.18: Spectrum of the motor current with two broken rotor bars and high load condition a)MCSA b)MSCSA

Finally, based on the data obtained, the table 6.1.3 presents the patterns selected for the detection of broken rotor bars.

Table 6.3: Detection patterns for Broken rotor bars

	MCSA			MSCSA		
	$(1+s)f_s$	$(1+2s)f_s$	$(1+3s)f_s$	$(1+s)2f_s$	$(1+2s)2f_s$	$(1+3s)2f_s$
Low load 1 Brb	5-10dB	0-5dB	0dB	5-10dB	3-7dB	0-5dB
High load 1 Brb	5-15dB	0-5dB	0dB	10-20dB	5-10dB	0-5dB
Low load 2 Brb	10-20dB	0-5dB	0-5dB	15-20dB	10-15dB	3-7dB
High load 2 Brb	10-25dB	5-10dB	0-5dB	20-30dB	10-20dB	5-10dB

6.1.4 Fuzzy Control

Once, after having performed the tests of eccentricity, broken rotor bars and voltage unbalance, it was possible to observe the variability presented in the amplitude and the frequency of the selected harmonics, depending on the motor specifications (rotor speed, power, torque, etc.) and the load level.
Based on this information, it was decided to perform a control with the use of the Fuzzy logic. This because, fuzzy controllers permit to work with variables that do not have a precise value, this means, that it is possible to couple the uncertainty into these variables. They are able to work in presence of noise, without ignoring the ability to manipulate variables based on the experience of the machine operator.

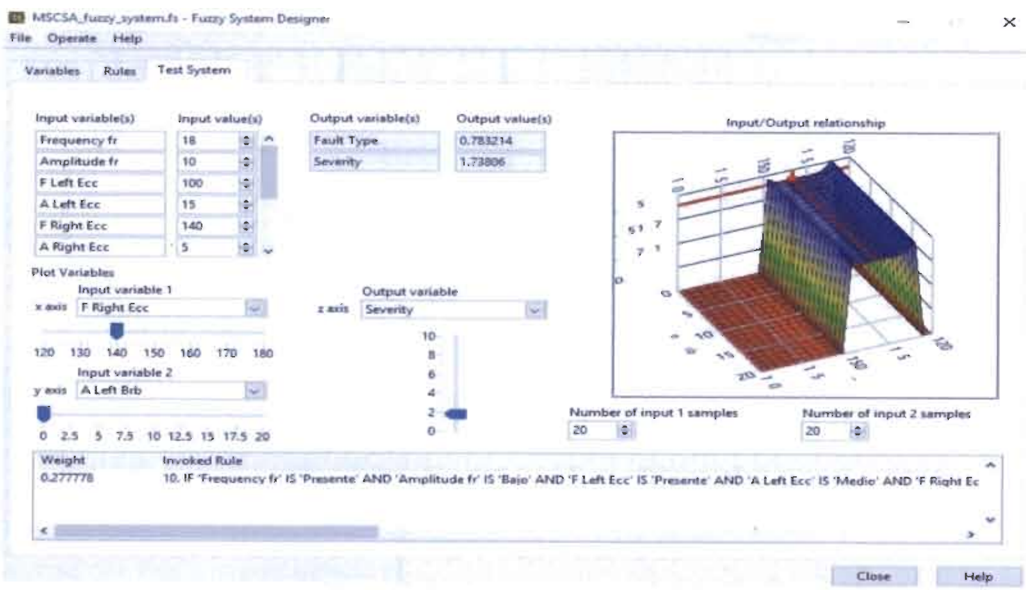

Figure 6.19: Fuzzy system (membership functions, rules and outputs)

Figure 6.19 presents the system to test the fuzzy controller developed. In the left side of the image the variables selected are presented and with them a value to test the input, respectively. In the bottom, depending on the values of the inputs, the activated rules are shown. In the center of the interface, the outputs obtained are displayed in a numerical way and in the right side in a graphical way.

Subsequently, after having highlighted the reasons why a fuzzy logic system was determined it was proceeded to establish the variables to manipulate, as well as, the membership functions for each of them.

It was established 6 input variables: frequency and amplitude of the selected harmonics (rotor frequency , sidebands on the left of the supply frequency and sidebands on the right of the supply frequency) and 2 output variables: Fault type and Severity of the fault. 6.19.

Membership functions are next described:

Inputs

Rotor frequency:

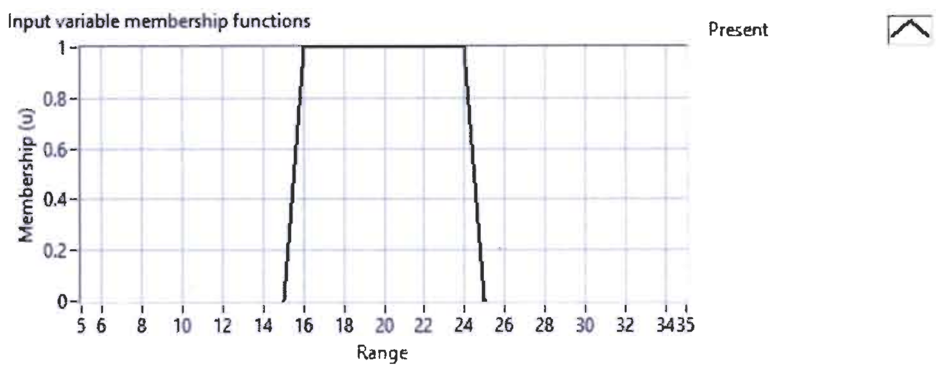

Figure 6.20: Membership functions of the rotor frequency

$$\mu_{f_r} = \begin{cases} 0 & if \quad x < 15 \\ x - 15 & if \quad 15 \leq x \leq 16 \\ 1 & if \quad 16 \leq x \leq 24 \\ 25 - x & if \quad 24 \leq x \leq 25 \\ 0 & if \quad x > 25 \end{cases} \tag{6.1}$$

Amplitude of the rotor frequency:

Figure 6.21: Membership functions for the amplitude of the rotor frequency

$$\mu_{A_{fr(low)}} = \begin{cases} 0 & if \quad x < 0 \\ x & if \quad 0 \leq x \leq 1 \\ 1 & if \quad 1 \leq x \leq 6 \\ \frac{15-x}{9} & if \quad 6 \leq x \leq 15 \\ 0 & if \quad x > 15 \end{cases} \tag{6.2}$$

$$\mu_{A_{fr(high)}} = \begin{cases} 0 & if \quad x < 5 \\ \frac{x-5}{9} & if \quad 5 \leq x \leq 14 \\ 1 & if \quad 14 \leq x \leq 20 \\ 0 & if \quad x > 20 \end{cases}$$

In the Figure 6.21 is shown the fuzzy set for the amplitude of the rotor frequency. In the figure it is possible to observe the membership functions for both states (Low amplitude in blue and High amplitude in green). The range of the values were determined in base of the results obtained and the membership degree based on the behavior of the variables.

Left sidebands frequency:

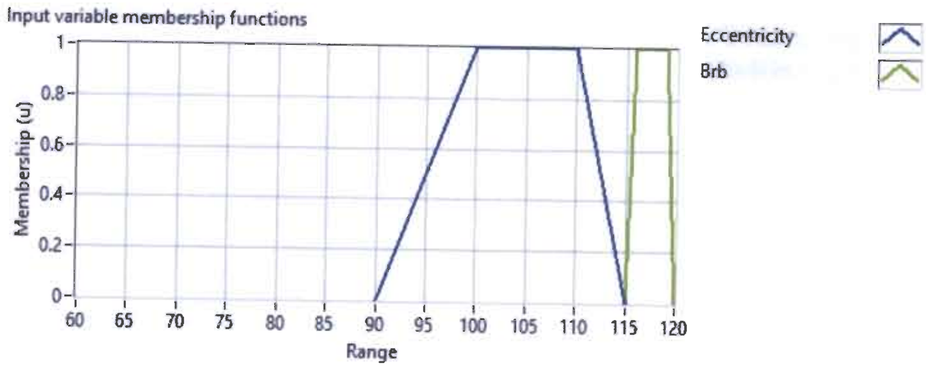

Figure 6.22: Membership functions for the frequencies on the left of the supply frequency

$$\mu_{f_{LSB_{Ecc}}} = \begin{cases} 0 & if \quad x < 90 \\ \frac{x-90}{10} & if \quad 90 \leq x \leq 100 \\ 1 & if \quad 100 \leq x \leq 110 \\ \frac{115-x}{5} & if \quad 110 \leq x \leq 115 \\ 0 & if \quad x > 115 \end{cases} \tag{6.3}$$

$$\mu_{f_{LSB_{Brb}}} = \begin{cases} 0 & if \quad x < 115 \\ x-115 & if \quad 115 \leq x \leq 116 \\ 1 & if \quad 116 \leq x \leq 119 \\ 120-x & if \quad 119 \leq x \leq 120 \\ 0 & if \quad x > 120 \end{cases}$$

Amplitude of the left sidebands harmonics:

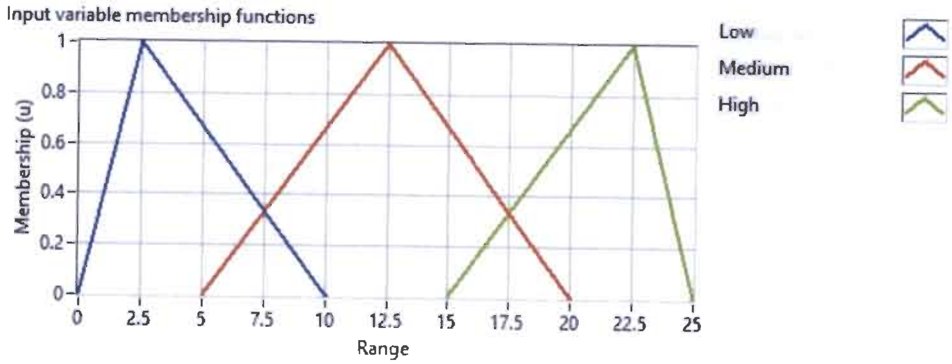

Figure 6.23: Membership functions for the amplitude of left side frequencies

$$\mu_{A_{LSB}(low)} = \begin{cases} 0 & if \quad x < 0 \\ \frac{x}{2.5} & if \quad 0 \leq x \leq 2.5 \\ \frac{10-x}{7.5} & if \quad 2.5 \leq x \leq 10 \\ 0 & if \quad x > 10 \end{cases} \tag{6.4}$$

$$\mu_{A_{LSB}(medium)} = \begin{cases} 0 & if \quad x < 5 \\ \frac{x-5}{7.5} & if \quad 5 \leq x \leq 12.5 \\ \frac{20-x}{7.5} & if \quad 12.5 \leq x \leq 20 \\ 0 & if \quad x > 20 \end{cases}$$

$$\mu_{A_{LSB}(high)} = \begin{cases} 0 & if \quad x < 15 \\ \frac{x-15}{7.5} & if \quad 15 \leq x \leq 22.5 \\ \frac{25-x}{2.5} & if \quad 22.5 \leq x \leq 25 \\ 0 & if \quad x > 25 \end{cases}$$

Right sidebands frequency:

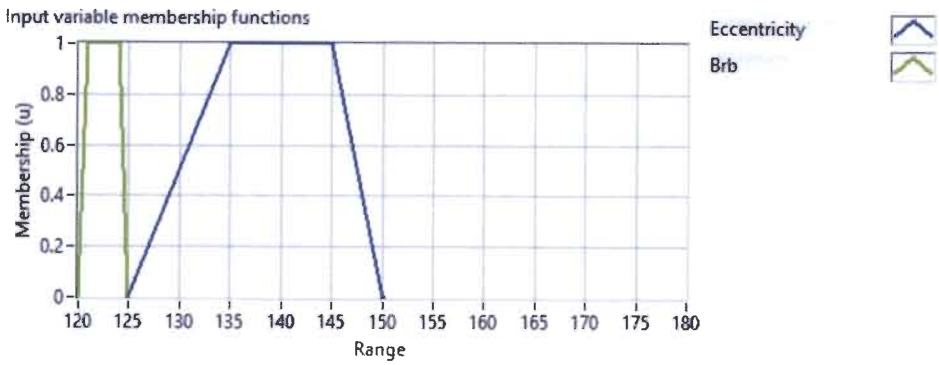

Figure 6.24: Membership functions for the frequencies on the right of the supply frequency

$$\mu_{f_{RSB_{Brb}}} = \begin{cases} 0 & if & x < 120 \\ x - 120 & if & 120 \leq x \leq 121 \\ 1 & if & 121 \leq x \leq 122 \\ \frac{125-x}{3} & if & 122 \leq x \leq 125 \\ 0 & if & x > 125 \end{cases} \tag{6.5}$$

$$\mu_{f_{RSB_{Ecc}}} = \begin{cases} 0 & if & x < 125 \\ \frac{x-125}{10} & if & 125 \leq x \leq 135 \\ 1 & if & 135 \leq x \leq 145 \\ \frac{150-x}{5} & if & 140 \leq x \leq 150 \\ 0 & if & x > 150 \end{cases}$$

Amplitude of the Right sidebands harmonics:

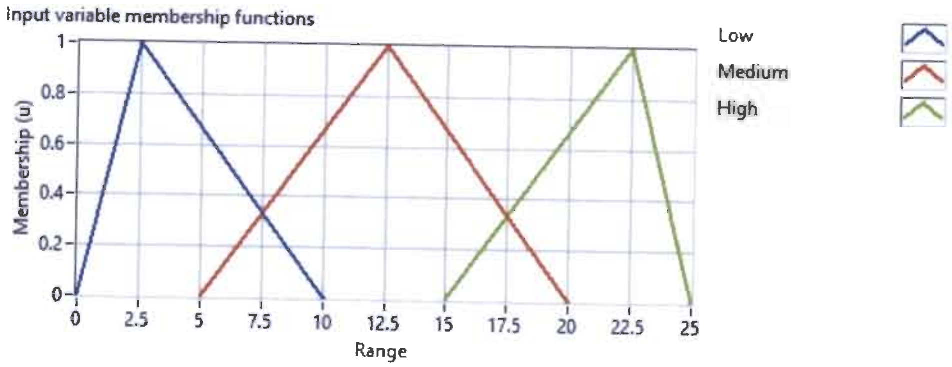

Figure 6.25: Membership functions for the amplitude of right side frequencies

$$\mu_{A_{RSB}(low)} = \begin{cases} 0 & if \quad x < 0 \\ \frac{x}{2.5} & if \quad 0 \leq x \leq 2.5 \\ \frac{10-x}{7.5} & if \quad 2.5 \leq x \leq 10 \\ 0 & if \quad x > 10 \end{cases} \tag{6.6}$$

$$\mu_{A_{RSB}(medium)} = \begin{cases} 0 & if \quad x < 5 \\ \frac{x-5}{7.5} & if \quad 5 \leq x \leq 12.5 \\ \frac{20-x}{7.5} & if \quad 12.5 \leq x \leq 20 \\ 0 & if \quad x > 20 \end{cases}$$

$$\mu_{A_{RSB}(high)} = \begin{cases} 0 & if \quad x < 15 \\ \frac{x-15}{7.5} & if \quad 15 \leq x \leq 22.5 \\ \frac{25-x}{2.5} & if \quad 22.5 \leq x \leq 25 \\ 0 & if \quad x > 25 \end{cases}$$

Outputs

Fault type:

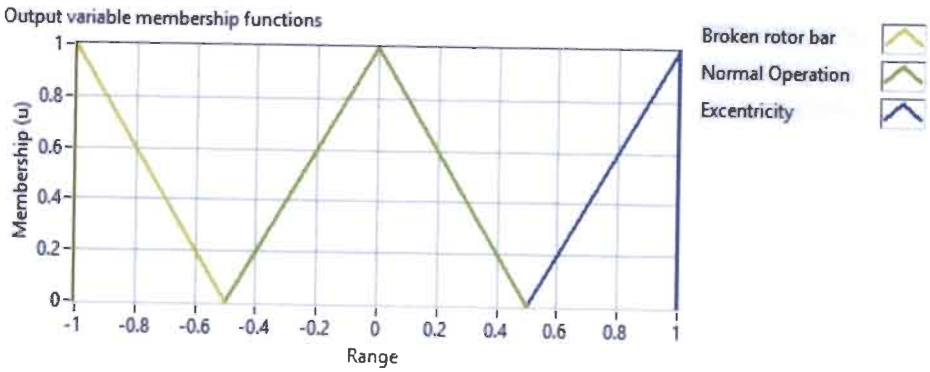

Figure 6.26: Membership functions for the output (Fault type)

$$\mu_{FT_{Brb}} = \begin{cases} 0 & if \quad x < -1 \\ 1 & if \quad x = -1 \\ \frac{-0.5-x}{0.5} & if \quad -1 \leq x \leq -0.5 \\ 0 & if \quad x > -0.5 \end{cases} \tag{6.7}$$

$$\mu_{FT_{NOM}} = \begin{cases} 0 & if \quad 0.5 < x < -0.5 \\ \frac{x+0.5}{0.5} & if \quad -0.5 \leq x \leq 0 \\ \frac{0.5-x}{0.5} & if \quad 0 \leq x \leq 0.5 \\ 0 & if \quad x > 0.5 \end{cases}$$

$$\mu_{FT_{Ecc}} = \begin{cases} 0 & if \quad x < 0.5 \\ 1 & if \quad x = 1 \\ \frac{x-0.5}{0.5} & if \quad 0.5 \leq x \leq 1 \\ 0 & if \quad x > 1 \end{cases}$$

Fault severity:

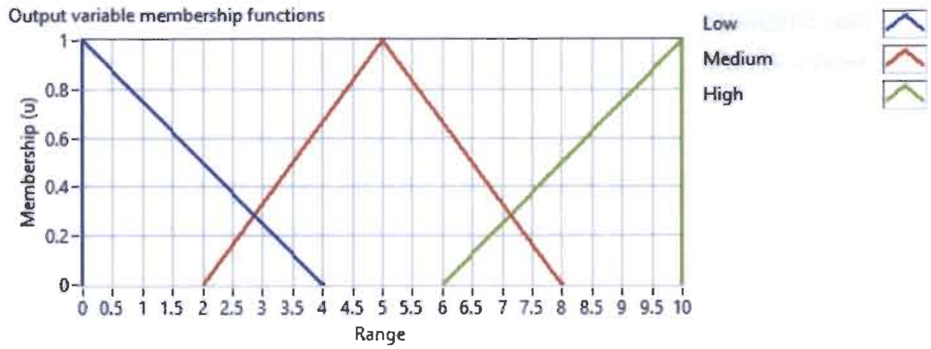

Figure 6.27: Membership functions for the output (Fault severity)

$$\mu_{FS_{low}} = \begin{cases} 0 & if \quad x < 0 \\ 1 & if \quad x = 0 \\ \frac{4-x}{4} & if \quad 0 \leq x \leq 4 \\ 0 & if \quad x > 4 \end{cases} \tag{6.8}$$

$$\mu_{FS_{medium}} = \begin{cases} 0 & if \quad 8 < x < 2 \\ \frac{x-2}{3} & if \quad 2 \leq x \leq 5 \\ \frac{8-x}{3} & if \quad 5 \leq x \leq 8 \\ 0 & if \quad x > 8 \end{cases}$$

$$\mu_{FS_{high}} = \begin{cases} 0 & if \quad x < 6 \\ 1 & if \quad x = 10 \\ \frac{x-6}{4} & if \quad 6 \leq x \leq 10 \\ 0 & if \quad x > 10 \end{cases}$$

Once defined the membership functions for the inputs and the outputs, it was proceeded to establish the rules to obtain the expected output. The total number of the generated rules were 24, a Mamdani max-min as inference engine and Center Of the Area (COA) as the defuzzification method. Below, the rules are exemplify:

- IF f_r is "present" and A_{f_r} is "low" and f_{LSB} is "Ecc" and A_{LSB} is "low" and f_{RSB} is "Ecc" and A_{RSB} is "low" and f_{LSB} is not "*Brb*" THEN Fault type is "Normal Operation Mode"
- IF f_r is "present" and A_{f_r} is "low" and f_{LSB} is "Ecc" and A_{LSB} is "low" and f_{RSB} is "Ecc" and A_{RSB} is "Medium" and f_{LSB} is not "*Brb*" THEN Fault type is "Normal Operation Mode"

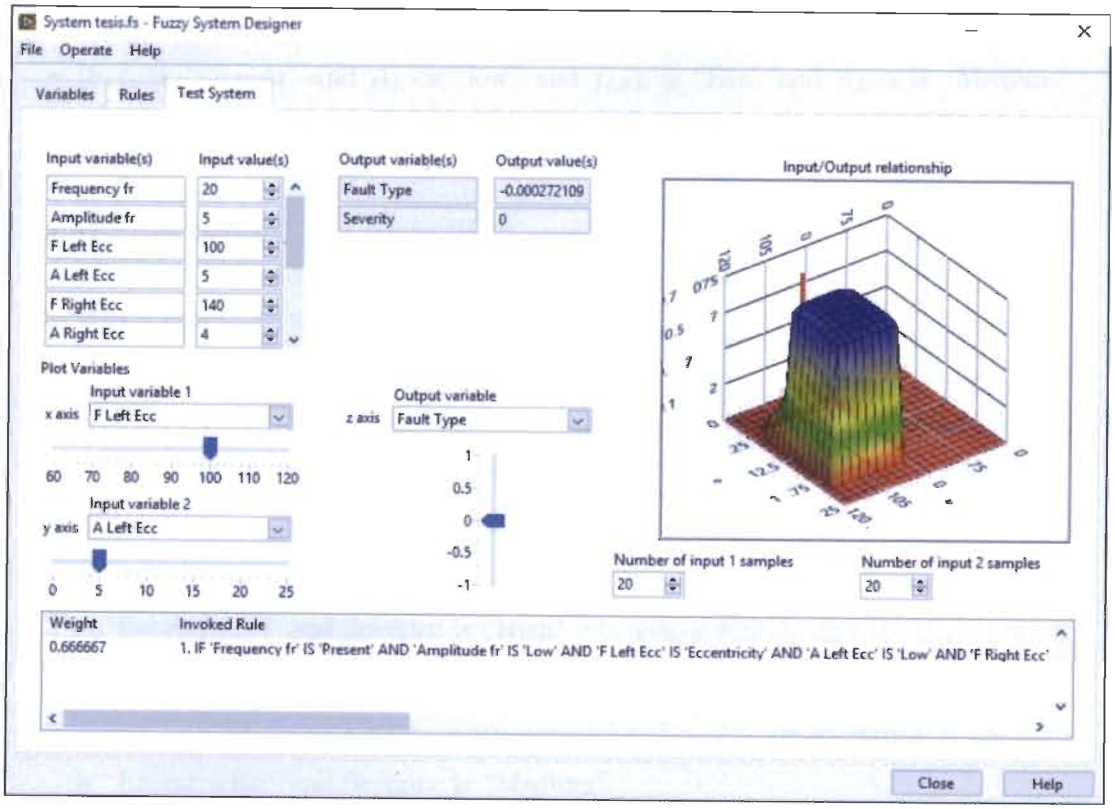

Figure 6.28: Example of the system in normal operation mode

Figure 6.28 presents the system under normal operation mode. It left side of the interface it is possible to observe that the harmonics for eccentricity fault are present. However, the amplitude of this harmonics are not significant to detect the fault.

- IF f_r is "present" and A_{f_r} is "low" and f_{LSB} is "Ecc" and A_{LSB} is "Medium" and f_{RSB} is "Ecc" and A_{RSB} is "medium" and f_{LSB} is not "*Brb*" THEN Fault type is "Eccentricity" and Severity is "Medium"

- IF f_r is "present" and A_{f_r} is "low" and f_{LSB} is "Ecc" and A_{LSB} is "High" and f_{RSB} is "Ecc" and A_{RSB} is "High" and f_{LSB} is not "*Brb*" THEN Fault type is "Eccentricity" and Severity is "Medium"

- IF f_r is "present" and A_{f_r} is "low" and f_{LSB} is "Ecc" and A_{LSB} is "Medium" and f_{RSB} is "Ecc" and A_{RSB} is "High" and f_{LSB} is not "*Brb*" THEN Fault type is "Eccentricity" and Severity is "Medium"

- IF f_r is "present" and A_{f_r} is "low" and f_{LSB} is "Ecc" and A_{LSB} is "Medium" and f_{RSB} is "Ecc" and A_{RSB} is "Low" and f_{LSB} is not "*Brb*" THEN Fault type is "Eccentricity" and Severity is "Low"

- IF f_r is "present" and A_{f_r} is "High" and f_{LSB} is "Ecc" and A_{LSB} is "Low" and f_{RSB} is "Ecc" and A_{RSB} is "Medium" and f_{LSB} is not "*Brb*" THEN Fault type is "Eccentricity" and Severity is "Low"

- IF f_r is "present" and A_{f_r} is "High" and f_{LSB} is "Ecc" and A_{LSB} is "Medium" and f_{RSB} is "Ecc" and A_{RSB} is "medium" and f_{LSB} is not "*Brb*" THEN Fault type is "Eccentricity" and Severity is "Medium"

- IF f_r is "present" and A_{f_r} is "High" and f_{LSB} is "Ecc" and A_{LSB} is "High" and f_{RSB} is "Ecc" and A_{RSB} is "Medium" and f_{LSB} is not "*Brb*" THEN Fault type is "Eccentricity" and Severity is "High"

- IF f_r is "present" and A_{f_r} is "High" and f_{LSB} is "Ecc" and A_{LSB} is "Medium" and f_{RSB} is "Ecc" and A_{RSB} is "High" and f_{LSB} is not "*Brb*" THEN Fault type is "Eccentricity" and Severity is "Medium"

- IF f_r is "present" and A_{f_r} is "High" and f_{LSB} is "Ecc" and A_{LSB} is "High" and f_{RSB} is "Ecc" and A_{RSB} is "High" and f_{LSB} is not "*Brb*" THEN Fault type is "Eccentricity" and Severity is "High"

- IF f_{LSB} is "Ecc" and A_{LSB} is "Medium" and f_{RSB} is "Ecc" and A_{RSB} is "medium" and f_{LSB} is not "*Brb*" THEN Fault type is "Eccentricity" and Severity is "Low"

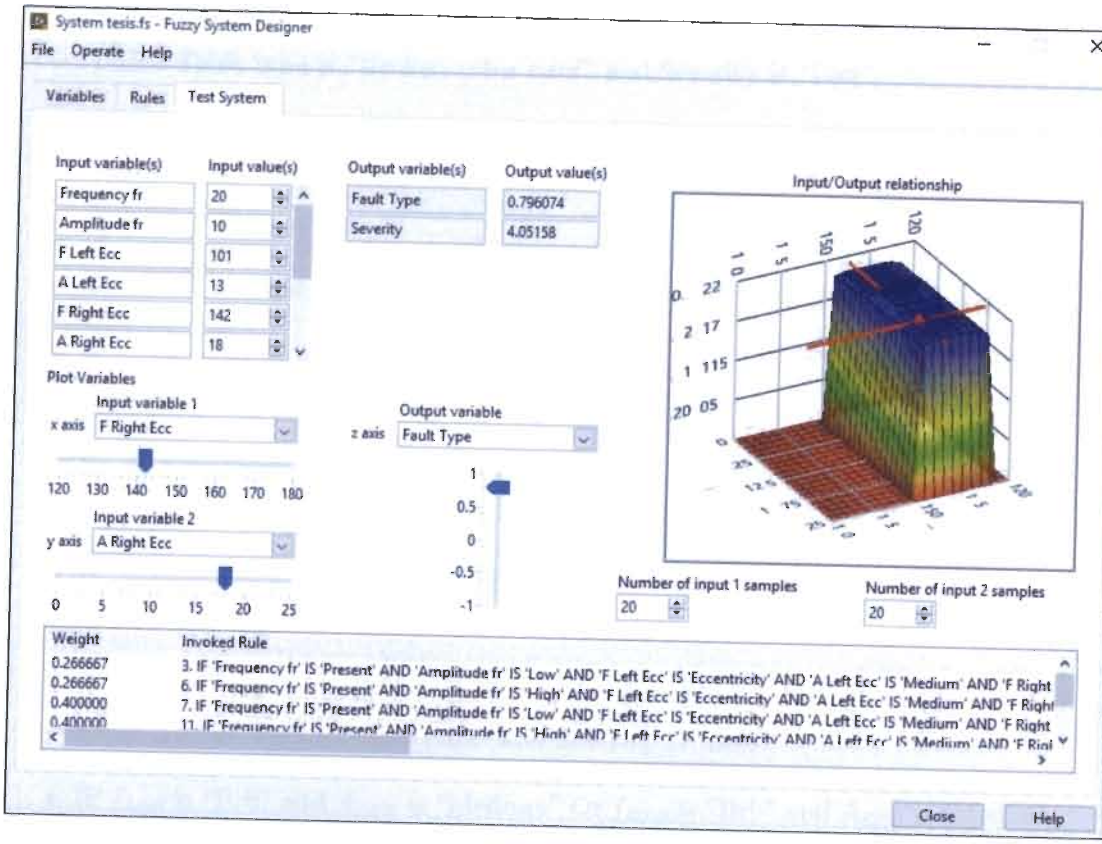

Figure 6.29: Example of the system with eccentricity fault

In the figure 6.29 the interface is tested for eccentricity faults. Observing the the bottom of the interface can be observed that in this case, the amplitude of the rotor frequency is located in the intersection of both membership functions (low and high severity). Given these conditions, 4 rules are fired obtaining as result an Eccentricity fault with a considerable severity.

- IF f_{LSB} is "Brb" and A_{LSB} is "Low" and f_{RSB} is "Brb" and A_{RSB} is "Low" THEN Fault type is "Broken rotor bars" and Severity is "Low"
- IF f_{LSB} is "Brb" and A_{LSB} is "Medium" and f_{RSB} is "Brb" and A_{RSB} is "Medium" THEN Fault type is "Broken rotor bars" and Severity is "Medium"

- IF f_{LSB} is "Brb" and A_{LSB} is "High" and f_{RSB} is "Brb" and A_{RSB} is "High" THEN Fault type is "Broken rotor bars" and Severity is "High"
- IF f_{LSB} is "Brb" and A_{LSB} is "Medium" and f_{RSB} is "Brb" and A_{RSB} is "Low" THEN Fault type is "Broken rotor bars" and Severity is "Low"
- IF f_{LSB} is "Brb" and A_{LSB} is "Low" and f_{RSB} is "Brb" and A_{RSB} is "Medium" THEN Fault type is "Broken rotor bars" and Severity is "Medium"
- IF f_{LSB} is "Brb" and A_{LSB} is "High" and f_{RSB} is "Brb" and A_{RSB} is "Medium" THEN Fault type is "Broken rotor bars" and Severity is "High"
- IF f_{LSB} is "Brb" and A_{LSB} is "Medium" and f_{RSB} is "Brb" and A_{RSB} is "High" THEN Fault type is "Broken rotor bars" and Severity is "High"
- IF f_{LSB} is "Brb" and A_{LSB} is "Low" and f_{RSB} is "Brb" and A_{RSB} is "High" THEN Fault type is "Broken rotor bars" and Severity is "Medium"
- IF f_{LSB} is "Brb" and A_{LSB} is "High" and f_{RSB} is "Brb" and A_{RSB} is "Low" THEN Fault type is "Broken rotor bars" and Severity is "Medium"
- IF f_{LSB} is "Brb" and A_{LSB} is "Low" Or f_{RSB} is "Brb" and A_{RSB} is "Low" THEN Fault type is "Broken rotor bars" and Severity is "Low"
- IF f_{LSB} is "Brb" and A_{LSB} is "Medium" Or f_{RSB} is "Brb" and A_{RSB} is "Medium" THEN Fault type is "Broken rotor bars" and Severity is "Medium"
- IF f_{LSB} is "Brb" and A_{LSB} is "High" Or f_{RSB} is "Brb" and A_{RSB} is "High" THEN Fault type is "Broken rotor bars" and Severity is "Medium"

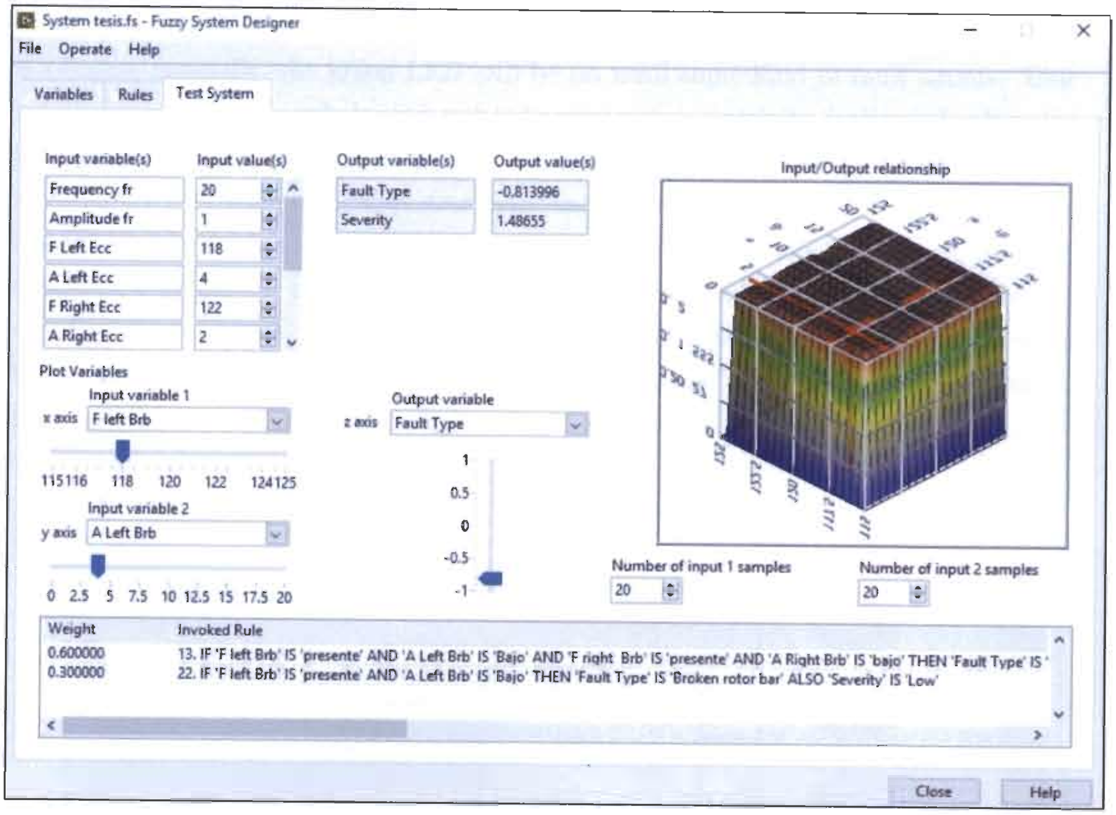

Figure 6.30: Example of the system with broken rotor bars

In the figure 6.30 is presented the interface tested for broken rotor bars. In this case, one point should be remarked; The harmonic of the rotor frequency is presented. However, the fault detected was broken rotor bars. This due the system was developed to detect broken rotor bars even when eccentricity harmonics are present. If both patterns are present, the eccentricity is taken as a consequence generated by the broken rotor bars.

Then, with the complete fuzzy controller defined, it was proceeded to perform several tests in order to evaluate the efficiency of the proposed methodology.

Figures 6.31 present the interface developed working. The interface is constituted by 4 principal parts. In the top left-hand corner it is shown the current obtained of one of the motor phases in time domain. In the bottom left-hand corner it is show the obtained current in frequency domain. The input variables for the fuzzy system are shown in the in the center at the bottom of the interface. Finally, in the right side of the interface it is shown the output of the system. This part of the interface presents on the left side 4 leds to indicate the operation of the system. if the motor is running normally, the green LED will be on until some kind of fault occurs. Blue led represents voltage unbalances, red led represents eccentricity faults and yellow led represents broken rotor bars. In the right side it is showed the severity of the fault in a scale of 0 to 10, being 0 the lowest severity and 10 the highest severity of the fault. In image "a" is possible to see the interface on normal operation mode, it can be observed certain harmonics on the multiples of the supply frequency. However, they are not significantly to detect a voltage unbalance. On the other hand, figure "b" presents the interface under voltage unbalance. Here, it is possible to see that the multiples harmonics, increase significantly indicating the presence of noise or a bad function on the supply current.

a)

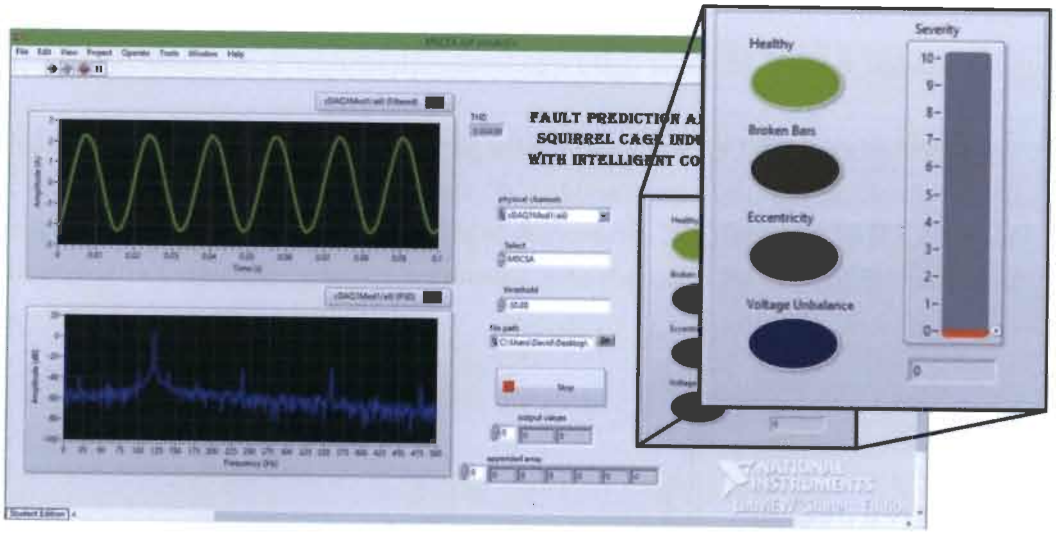

b)

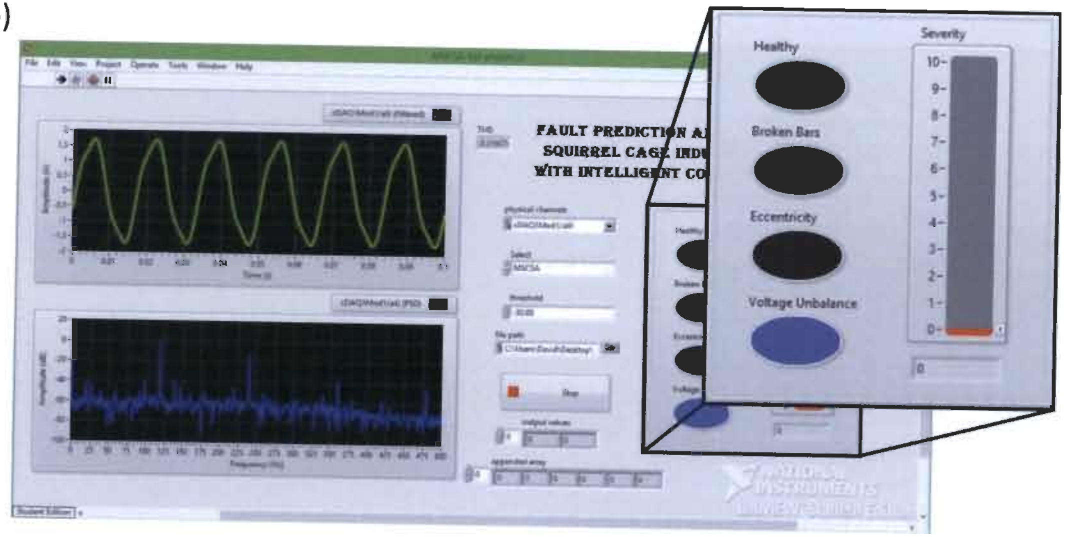

Figure 6.31: Interface developed a)Normal operation mode b) Voltage unbalance

Figure 6.32 shows the interface working with an eccentricity fault , under low severity (Figure "a") and high severity (Figure "b"). Observing both figures, it can be observed that both faults present harmonics at frequencies 20, 100 and 140 Hz, however the difference in amplitude between harmonics, sets the norm for the determination of the severity of the fault.

a)

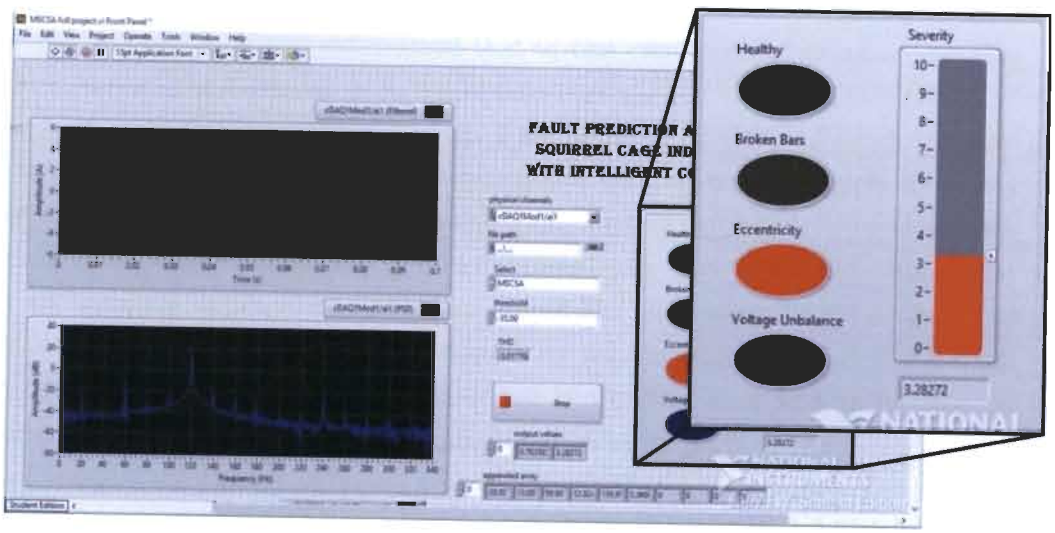

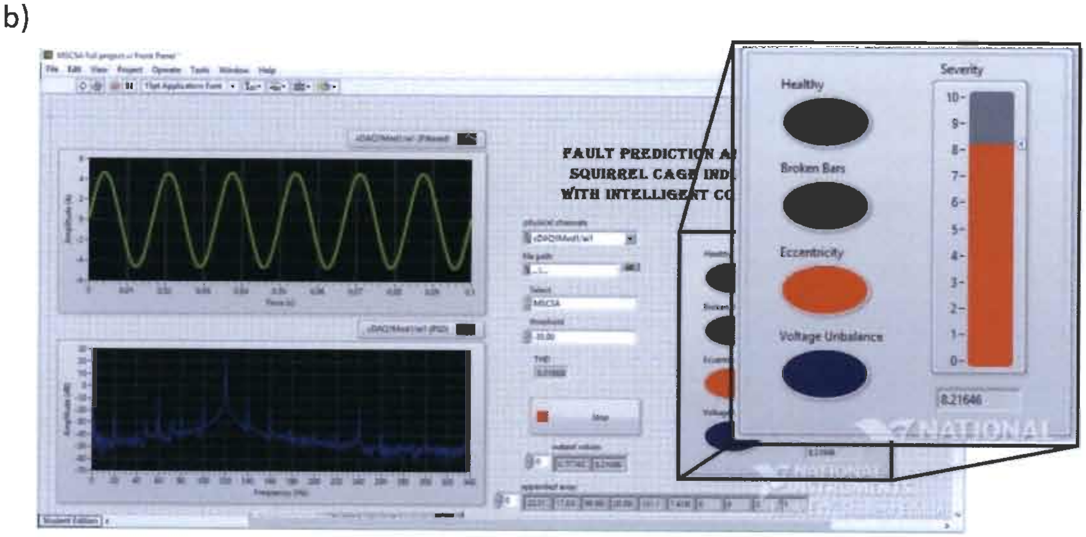

Figure 6.32: Interface working with Eccentricity Fault a)Low severity b) High severity

Finally, the last validation was made with broken rotor bars. Figures 6.33 present the graphics and the outputs obtained by the analysis with one and two broken bars. There are two points to note about the determination of the level and severity of faults. First, as in eccentricity, it is possible to see, how the severity of the fault is directly affected by the amplitude of the selected harmonics $(1 \pm s)2f_s$. The second point to observe, is about the highlighting harmonics. If the graphic is watched more closely, it can be noted the presence of the eccentricity harmonics at $2f_s \pm f_r$. However, after the performed proofs, it was determined that in this case, even when an eccentricity could be present, the causative of it, are broken bars.

In this fault, one point should be remarked. If the figure "a" is observed closer, it is possible to note that the amplitude of the harmonics on both sides of the supply frequency presents a short value comparatively with the presented on figure "b", however on both cases the alarm was activated. In the case of broken rotor bars, it was determined that when an harmonic appears, no matter his amplitude, the system would activate the alarm for broken rotor bars (unlike to eccentricity failures which were allowed a small clearance). This is because a broken rotor bar is a critical fault and an increase on the severity of this fault could cause higher fault in other parts of the motor. In the case of eccentricity, these conditions are not presented, this is due different external elements like couplings could cause a small unbalance, representing a little variation on the signal obtained.

a)

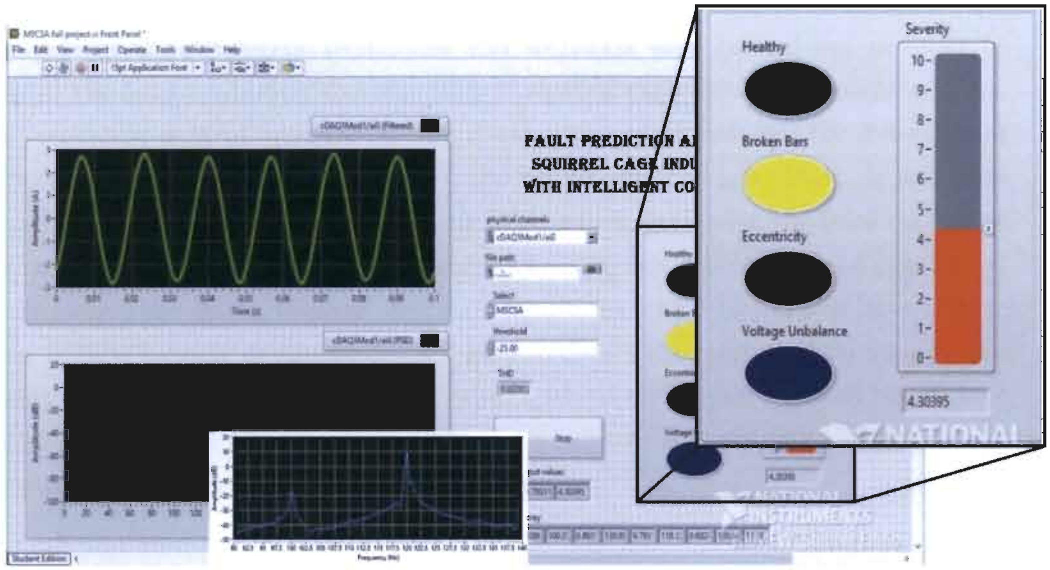

b)

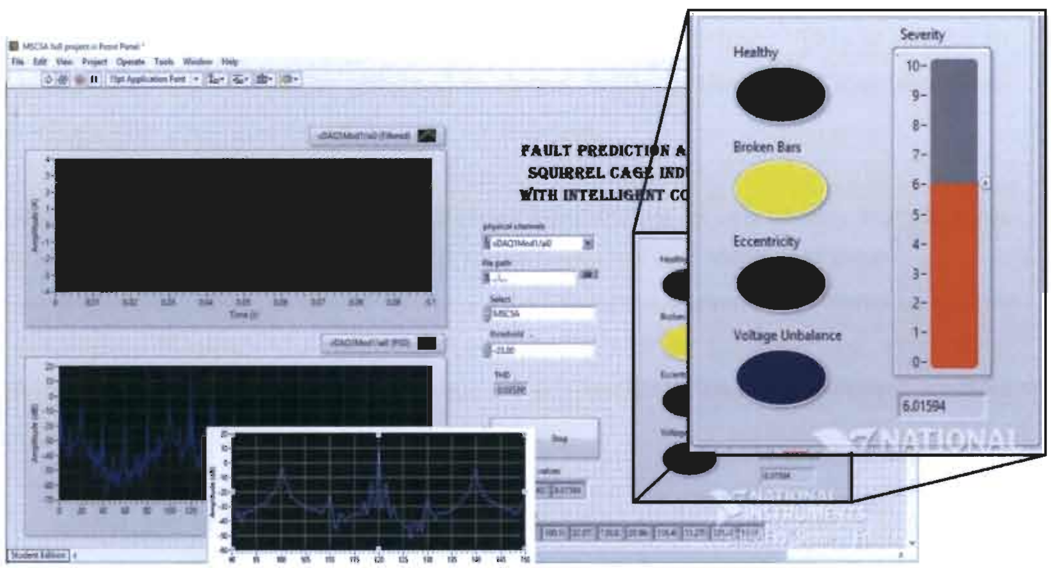

Figure 6.33: Interface working with Broken Rotor Bars a)Low severity b) High severity

6.2 Discussion

In the present work different techniques and scenarios were carried out in order to determine the fault prediction and diagnosis in squirrel cage induction motors with the use of intelligent control systems. It was developed several tests for the detection of both faults, electrical (broken rotor bars), and mechanical (eccentricities). It was been observed that techniques such as MCSA or ESA, which work with the pure current of one of the motor phases, allow good detection when the motor is on full load conditions. However, when the motor is under low load conditions, these techniques have a large number of false alarms, or simply are not able to detect the fault. In this regard, it is necessary to make the combination with other analysis techniques (such as the Hilbert transform) in order to amplify these patterns to increase the sensibility of the system making it able to work under low load conditions.

The results with MCSA technique was observed that the patterns presented under full load conditions, were presented in greater numbers, making it more efficient than techniques like MCSA or ESA. Moreover, the biggest advantage of this technique was that MSCSA had no problem working under low load conditions. This is due to in those conditions, the resolution obtained to detect faults in the motor was improved, even without the combination with other techniques.

Regarding to techniques used for pattern classification is concerned, several tests to different techniques such as PCA, and fuzzy logic systems were performed.
The use of the technique such as PCA presented favourable results in terms of simple fault detection. However the technique presented problems for detection when multiple failures occurred. This problem was solved, with the use of intelligent control techniques such as Fuzzy Logic Control systems.

The advantages of the MSCSA technique for signal analysis and Fuzzy Logic technique for pattern classification were used to propose a methodology to detect and diagnose faults in squirrel cage induction motors that consists basically into 5 steps:

- Adquisition of the current on one of the motor phases.
- Preprocess of the signal in order to transform from time domain to frequency domain
- Acquire information about the selected harmonics.

- Based on the information obtained (frequency and amplitude), diagnose the motor state with the use of a Fuzzy controller.
- Provide an appropiate solution based on the fault type and the severity.

This methodology was proved on simulation and validated into 2 squirrel cage induction motors .

One of the drawbacks noted in the literature as much as in practice, was that tests were performed on controlled conditions, this means, that there was no possibility to present false alarms caused by a fault on the supply network, or an unbalance generated by external vibrations on the process, conditions that are very frequently presented in the industry, also known as industrial noise.

For the fault simulation on the supply network, several proofs were performed to identify voltage unbalance and with that, known the quality of the current of the motor. With this analysis, a new pattern was selected, the total harmonic distortion. Based on this, different levels of operation were established, if the THD is higher than 10 %, the fault may be caused by a fault on the power supply. Thus, the system will be able to work with noise presence, fulfilling the second objective proposed.

Finally, based on the results obtained it is possible to conclude the next:

The technique MCSA is a powerful technique for the detection of eccentricity faults and broken rotor bars under normal load conditions. However at the moment when the motor is working under low load conditions, the technique presents problems to make a correct diagnosis of the fault, and it is necessary to use other techniques to improve the resolution of the system. On the other hand, the MSCSA technique uses the square of the current in order to improve the resolution of the system, obtaining as a result, a tool with a better performance for the detection and diagnosis of faults without the use of an additional technique.

Tests for eccentricity faults showed the robustness of the technique for the detection of this fault. The technique presented a high sensibility for the detection, even on difficult scenarios (like low load and presence of external vibrations). However, one point to consider is that the coupling of external elements such as bushings, can provoke unbalance on the shaft. This problem generates low amplitude harmonics in the signal analysis, causing problems with false alarms. To avoid these problems, a clearance was introduced into the control system in order to avoid false alarms. Once added the clearance, the number of false alarms were practically nullified.

For broken rotor bars, results showed that, even when the MSCSA improve the resolution of the technique to make the system able to work under low load conditions, the detection of broken rotor bars gets complicated when the motor is under no load condition. However, to avoid such faults, an easy installation system for simulating load to the motor was created in order to generate a robust system for the detection of faults.

Other point observed after the tests, was the presence of eccentricity patterns on the frequency analysis. Two possible answers were defined for this event. The first and most probable of them, is that at the moment of holes were drilled to break the rotor bars, a weight unbalance was generated causing faults by eccentricity. The second one is that the shortcircuit caused by the broke of the rotor bars, generates fluctuations in the magnetic field causing problems by eccentricity in the motor. Regardless, as both reasons are caused by the broken bars, in the system was established that in presence of both patterns (eccentricity and broken rotor bars), the system generates an alarm corresponding for broken rotor bars.

After having analyzed the classifying patterns and the behavior of the system, it looked for a technique able to work with ambiguous variables and to establish of control parameters. Based on these characteristics, it was decided to use a fuzzy logic system. Fuzzy system allows to perform a control system taking in count the variables based on the experience of the process. Also it is possible to work in the presence of uncertainty, which in the case of the analysis of the motors, presents a great advantage. The results obtained for this technique showed a correct diagnosis when detecting eccentricities and broken bars. In addition, one of the main advantages of this technique was the correct diagnosis of faults, even when both faults were present. .

Finally based on the results obtained, it is possible to confirm the creation of an analysis, monitoring and control system, which by analyzing the current with the technique MSCSA and working together to a fuzzy logic system, is able to detect both faults, mechanical, caused by eccentricities and electrical, caused by broken bars in the rotor. Is worth to highlight that the system has the ability to work online, thus avoiding shutdowns on the line for analysis and diagnosis and also, it is qualified to work with the presence of noise (both electrical and mechanical). thus giving answer to the hypothesis proposed.

References

[1] C. J. V. G. G. Acosta and S. M. Ieee, "Técnicas de Detección y Diagnóstico de Fallos en Máquinas Eléctricas de Inducción," vol. 5, no. 1, pp. 41–49, 2007.

[2] C. R. Alavala, *Fuzzy Logic and Neural Networks (basic concepts & applications)*. 2008.

[3] S. Guedidi, S. E. Zouzou, W. Laala, M. Sahraoui, and K. Yahia, "Broken bar fault diagnosis of induction motors using MCSA and neural network," *SDEMPED 2011 - 8th IEEE Symposium on Diagnostics for Electrical Machines, Power Electronics and Drives*, no. 1, pp. 632–637, 2011.

[4] M. R. Mehrjou, N. Mariun, M. Hamiruce Marhaban, and N. Misron, "Rotor fault condition monitoring techniques for squirrel-cage induction machine - A review," *Mechanical Systems and Signal Processing*, vol. 25, pp. 2827–2848, Nov. 2011.

[5] P. Neti, "Electrical Signature Analysis Based Online Monitoring of Drive-trains for Doubly-fed Wind Generators," pp. 1764–1769, 2012.

[6] R. O. A. Gheitasi, M. Moghavvemi, "Speed variant motor fault diagnosis applying significant frequency bands," *2009 IEEE Student Conference in Research and Development*, pp. 353–356, November 2009.

[7] P. Neti, M. R. Shah, K. Younsi, J. Krahn, J. Y. Zhou, and C. D. Whitefield, "Motor current signature analysis during accelerated life testing of form wound induction motors," *Proceedings of the 2010 IEEE International Power Modulator and High Voltage Conference, IPMHVC 2010*, pp. 106–109, 2010.

[8] A. F. R. Maestre, *Deteccion de Fallas en un Motor de Induccion Usando MCSA (Motor Current Signature Analysis)*. PhD thesis, Universidad Industrial de Santander, 2011.

[9] B. Rajalakshmi Samaga and K. Vittal, "Comprehensive study of mixed eccentricity fault diagnosis in induction motors using signature analysis," *International Journal of Electrical Power & Energy Systems*, vol. 35, pp. 180–185, Feb. 2012.

[10] R. Kumar, K. Ray, and K. Kumar, "Fault diagnosis of industrial drives using MCSA techniques," *2009 International Conference on Control, Automation, Communication and Energy Conservation*, no. June, pp. 1–7, 2009.

[11] J. Rangel-magdaleno and J. Ramirez-cortes, "Broken Bars Detection on Induction Motor Using MCSA and Mathematical Morphology : An Experimental Study," no. x.

[12] C. Bruzzese, O. Honorati, and E. Santini, "Spectral Analyses of Directly Measured Stator and Rotor Currents for Induction Motor Bar Breakages Characterization by M . C . S . A .," pp. 6–11, 2006.

[13] K. V. Kumar, S. S. Kumar, and S. D. Stallon, "Experimental Verification of Squirrel Cage Induction Motor Using Current Signature and Virtual Instrumentation Topology," vol. 2012, no. Icsip 2012, pp. 477–486.

[14] S. Bindu and V. V. Thomas, "Diagnoses of internal faults of three phase squirrel cage induction motor - A review," *2014 International Conference on Advances in Energy Conversion Technologies - Intelligent Energy Management: Technologies and Challenges, ICAECT 2014*, pp. 48–54, 2014.

[15] M. Benbouzid, M. Vieira, and C. Theys, "Induction motors' faults detection and localization using stator current advanced signal processing techniques," *IEEE Transactions on Power Electronics*, vol. 14, no. 1, pp. 14–22, 1999.

[16] J. Puche-Panadero, R. ; Dept. of Electr. Eng., Univ. Politec. de Valencia, Valencia ; Pineda-Sanchez, M. ; Riera-Guasp, M. ; Roger-Folch and M. Authors, "Improved Resolution of the MCSA Method Via Hilbert Transform , Enabling the Diagnosis of Rotor Asymmetries at Very Low Slip," *IEEE TRANSACTIONS ON ENERGY CONVERSION*, vol. 24, no. 1, pp. 52–59, 2013.

[17] S. Ben Salem, K. Bacha, and M. Gossa, "Induction motor fault diagnosis using an improved combination of Hilbert and Park transforms," *2012 16th IEEE Mediterranean Electrotechnical Conference, MELECON 2012*, pp. 1141–1146, 2012.

[18] J. H. Jung, J. J. Lee, and B. H. Kwon, "Online diagnosis of induction motors using MCSA," *IEEE Transactions on Industrial Electronics*, vol. 53, no. 6, pp. 1842 1852, 2006.

[19] M. Sahraoui, S. E. Zouzou, A. Ghoggal, S. Guedidi, and H. Derghal, "An Improved Algorithm for Detection of Rotor Faults in Squirrel Cage Induction Motors Based on a New Fault Indicator," pp. 1572 1578, 2012.

[20] S. B. Chaudhury and S. Gupta, "Online identification of AC motor misalignment using current signature analysis and modified K-mean clustering technique," *Proceedings of the IEEE International Conference on Industrial Technology*, pp. 2331 2336, 2006.

[21] S. Guedidi, S. E. Zouzou, W. Laala, K. Yahia, and M. Sahraoui, "Induction motors broken rotor bars detection using MCSA and neural network: experimental research," *International Journal of System Assurance Engineering and Management*, vol. 4, pp. 173 181, Mar. 2013.

[22] H. S. Nur Aisyah Nordin, "Detection and Classification of Induction Motor Faults Using Motor Current Signature Analysis and Multilayer Perceptron," no. March, pp. 35 40, 2014.

[23] L. A. Pereira, S. Gazzana, and L. F. A. Pereira, "Motor Current Signature Analysis and Fuzzy Logic Applied to the Diagnosis of Short-Circuit Faults in Induction Motors," pp. 275 280, 2005.

[24] S. Zouzou, W. Laala, S. Guedidi, and M. Sahraoui, "A Fuzzy Logic Approach for the Diagnosis of Rotor Faults in Squirrel Cage Induction Motors," *2009 Second International Conference on Computer and Electrical Engineering*, vol. 2, pp. 173 177, 2009.

[25] R. Samaga and K. Vittal, "Effect of unbalance in voltage supply on the detection of mixed air gap eccentricity in an induction motor by Motor Current Signature Analysis," *ISGT2011-India*, pp. 108 113, 2011.

[26] A. I. Shady S. Refaat, Haitham Abu-Rub, "Ann-based system for discrimination between unbalanced supply voltage and phase loss in induction motors," *Machines and Drives (PEMD 2014) 7th IET internation Conference on Power Electronics*, pp. 1 6, March 2014.

[27] A. L. a. Fonseca, J. a. Lambert, R. V. a. Monteiro, A. B. D. Vasconcellos, and B. C. Carvalho, "Behavioral and Statistical Analysis of Total Harmonic Distortion Input Frequency Converter of a Triggering an Industrial Fan : A Case Study ..," *Behavioral and Statistical Analysis of Total Harmonic Distortion Input Frequency Converter of a Triggering an Industrial Fan: A Case Study.*, pp. 152–156, 2014.

[28] V. F. Pires, M. Kadivonga, J. F. Martins, and a. J. Pires, "Motor square current signature analysis for induction motor rotor diagnosis," *Measurement: Journal of the International Measurement Confederation*, vol. 46, pp. 942–948, Feb. 2013.

[29] S. J. Chapman, *Maquinas Electricas*. 2000.

[30] E. Castillo Pedrosa, Juan; Marrufo González, "Motores Eléctricos," in *Instalaciones eléctricas basicas. Grado medio- McGraw-Hill*, vol. 1, ch. 11, Mc. Graw Hill Companies, 2014.

[31] A. V. Flores, *Manual Motores Eléctricos*. Ingeniero Civil Eléctrico, Pages 1-70.

[32] L.-X. Wang, *A COURSE IN ' FUZZY A Course in Fuzzy Systems and Control*. 1997.

[33] I. Y. G. Math H.J. Bollen, *Signal Processing of Power Quality Disturbances*. John Wiley & Sons, Inc., 2006.

[34] M. Orman, M. Orkisz, and C. T. Pinto, "Slip estimation of a large induction machine based on MCSA," *SDEMPED 2011 - 8th IEEE Symposium on Diagnostics for Electrical Machines, Power Electronics and Drives*, pp. 568–572, 2011.

[35] G. Didier, E. Ternisien, O. Caspary, and H. Razik, "A new approach to detect broken rotor bars in induction machines by current spectrum analysis," *Mechanical Systems and Signal Processing*, vol. 21, pp. 1127–1142, Feb. 2007.